Environmental Modelling and Software 176 (2024) 106027

Contents lists available at ScienceDirect

Environmental Modelling and Software

journal homepage: www.elsevier.com/locate/envsoft

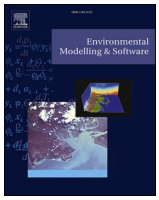

CyTRACK: An open-source and user-friendly python toolbox for detecting and tracking cyclones

Albenis Pérez-Alarcón [a,b,c,*], Patricia Coll-Hidalgo [a], Ricardo M. Trigo [c,d], Raquel Nieto [a], Luis Gimeno [a]

[a] Centro de Investigación Mariña, Universidade de Vigo, Environmental Physics Laboratory (EPhysLab), Campus As Lagoas s/n, 32004, Ourense, Spain
[b] Departamento de Meteorología, Instituto Superior de Tecnologías y Ciencias Aplicadas, Universidad de La Habana, 10400, La Habana, Cuba
[c] Instituto Dom Luiz (IDL), Facultade de Ciências, Universidade de Lisboa, 1749-016, Lisboa, Portugal
[d] Departamento de Meteorologia, Universidade Federal do Rio de Janeiro, Rio de Janeiro, 21941-919, Brazil

ARTICLE INFO

Keywords:
Cyclones
Detection and tracking
Python
Reanalysis dataset
Climate models

ABSTRACT

This work introduces CyTRACK (Cyclone TRACKing framework), a new open-source, comprehensive and user-friendly Python toolbox for detecting and tracking cyclones in model and reanalysis datasets. The kernel of CyTRACK is based on detecting critical cyclone centres in the mean sea level pressure field at a single time slice, which are then filtered following several threshold parameters. This paper also compares ten years of CyTRACK outputs forced with the ERA5 reanalysis against best-track archives and available cyclones track datasets. The results reveal that CyTRACK can capture the inter-annual (year to year) and intra annual (seasonal cycle) variability of cyclone frequency, life cycle characteristics and spatial distribution of track densities. Largest differences were observed in the annual and seasonal frequency. In summary, CyTRACK provides a user-friendly framework for sensitivity analysis of several free parameters used to perform the tracking, and it is useful for case or climatological studies of cyclone features.

1. Introduction

Atmospheric studies are increasingly based on improved numerical simulations concerning spatial and temporal resolution, initialization inputs, and complex environmental interactions. Climatological assessments, as well as specific events of cyclonic systems have been thoroughly studied by the scientific community due to their impacts on people's life. This widespread interest includes subtropical (SCs), tropical (TCs) and extratropical (ECs) cyclones, as their occurrence modulates regional and local weather regimes (Bevacqua et al., 2020; da Rocha et al., 2019; Flaounas et al., 2022; Hawcroft et al., 2012; Hofsteenge et al., 2022; Quinting et al., 2018). Additionally, they are involved in the exchange and redistribution of physical and thermodynamical properties (Albert et al., 2023; Munsi et al., 2022; Sinclair and Dacre, 2019; Shen and Zhang, 2022; Uotila et al., 2013; Yang et al., 2023), as well as in significant aspects of humankind's evolution in its quest for adaptation and resilience in the face of frequent extreme events (Baker et al., 2019; Lai et al., 2021; Pérez-Alarcón et al., 2023a; Yamaguchi et al., 2020). In recent decades there have been various efforts to detect the centres and establish the trajectories of these systems on reanalysis and modelling output datasets (see Neu et al., 2013; Ullrich and Zarzycki, 2017, and references therein). Accurately detecting and tracking in a gridded dataset largely depends on the threshold parameters that best describe cyclones, and there is no constraint framework for it.

Best-track databases could be a reasonable benchmark for automated cyclone detection and tracking methods (CDTMs) in model outputs, for both weather forecast and climate modeling. However, these databases have been largely developed for TCs (Knapp et al., 2010; Landsea and Franklin, 2013; Lu et al., 2021; Ying et al., 2014). For extratropical cyclones, the best-track methodologies can become more complex due to the wide range of EC's properties to be considered, i.e., shape symmetry, size, distinguishable centres, translation velocities, genesis precursors, and split/merge of features (Neu et al., 2013). Hence, benchmarking the performance of CDTMs remains difficult. Nevertheless, inter-comparison is a practice to determine the biases in the extratropical climatologies obtained through CDTMs, both in reanalysis data and high-resolution modelling. Recently, Flaounas et al. (2023)

* Corresponding author. Centro de Investigación Mariña, Universidade de Vigo, Environmental Physics Laboratory (EPhysLab), Campus As Lagoas s/n, 32004, Ourense, Spain.
E-mail address: albenis.perez.alarcon@uvigo.es (A. Pérez-Alarcón).

https://doi.org/10.1016/j.envsoft.2024.106027
Received 18 January 2024; Received in revised form 10 March 2024; Accepted 20 March 2024
Available online 21 March 2024

produced high-confidence datasets for the Mediterranean cyclones (MCs) based on the recent ERA5 reanalysis (Hersbach et al., 2020) by combining overlapping tracks from ten different CDTMs.

From the similarities and differences between CDTMs, the optimal algorithm selection mostly relies on the specific investigation goals. In this sense, previous authors documented consistent/discrepancies in applying different algorithms to the same input data (e.g., Horn et al., 2014; Neu et al., 2013; Raible et al., 2008) or one algorithm to different datasets (e.g., Bourdin et al., 2022; Gramcianinov et al., 2020; Malakar et al., 2020; Tilinina et al., 2013; Wang et al., 2016). Neu et al. (2013) noted that consistency between methods increased for well-developed cyclones, while the most considerable discrepancies were found for the detection and cyclone frequencies of weak systems. Similarly, when comparing three distinct algorithms, Raible et al. (2008) found differences in the number of cyclones, despite the consensus on inter-annual variability. Tracking methods differences between the datasets exhibited decreasing divergences when comparing recent periods (Gramcianinov et al., 2020; Bié and de Camargo, 2023), probably due to the amount and quality of assimilated observations (Wang et al., 2016). For both TCs and ECs, the authors agree that the errors in track in reanalysis datasets reduce with the system's intensification. In addition, Malakar et al. (2020) concluded that high-resolution downscaling is essential for inner core structure representation and description of the TC intensification process. Several annotations from research focused on tracking cyclonic systems in high-resolution data (e.g., Cattiaux et al., 2020; Marchok, 2021; Raavi and Walsh, 2020; Rohrer et al., 2020; Zarzycki et al., 2021) remark that Eulerian tracking methods are robust to changes in resolution, while Lagrangian tracking algorithms are largely dependent on it.

The objective and automatic Lagrangian CDTMs tools (so-called trackers) have streamlined this critical step for research purposes and forecasting services. One of their advantages relies on key characteristics such as "variable used" (Tory et al., 2013a; Walsh et al., 2007). The trackers generally split the problem into two stages: searcher cyclones-indicatives and pairing across time steps. In addition, implementation can vary across the computation of anomalies in a data field, identification of local extrema, and determination of closed contours or thresholds around a particular point (Ullrich and Zarzycki, 2017). Internally, a succession of rules and parameters are declared (as well as the criteria hierarchy) to discard false positives; at this point, the detection criteria and thresholds are suitable for the tracker. This flexibility, in combination with minor adjustments, permits that occasionally a tracker based on an algorithm for ECs (e.g. TRACK, Hodges, 1994, 1995, 1999) is adapted and used in tropical systems (e.g. Hodges et al., 2017; Roberts et al., 2020). Other software tools reach versatility when achieving robust applicability by avoiding issues associated with unstructured grids, split/merge features, small-scale noise or data singularity at the poles (e.g., "esd'' R-package, Benestad and Chen, 2006; CycloTRACK, Flaounas et al., 2014; TRI_TRACKER, Massey, 2016; TempestExtremes, Ullrich et al., 2021; TITAM, Pravia-Sarabia et al., 2020). Tracker kernel optimization is critical to the confidence level of the derived data (Bourdin et al., 2022).

Accordingly, it is fair to state that cyclone track software development is still an ongoing task. The variety of these methods will be as great as the evolution in the capacity of algorithms to capture the life cycle of systems and the emerging advances in the infrastructure of applications. It is also important to remark that the explosion of machine learning methods will likely further expand the number of fast and reliable cyclone tracking algorithms (Kumler-Bonfanti et al., 2020; Giffard-Roisin et al., 2020; Accarino et al., 2023). Despite the large number of methodologies to detect and track cyclones (see Neu et al., 2013; Ullrich and Zarzycki, 2017; Murata et al., 2019; Flaounas et al., 2023, and references therein), to the best of our knowledge, there is a limited number of tracker implementation or free availability codes for the scientific community. For example, the Centre for Earth Observation Science/National Snow and Ice Data Center Extratropical Cyclone Tracking (CNECT; Crawford and Serreze, 2016; Crawford et al., 2021), Stormtracks (https://github.com/markmuetz/stormtracks) and the National Oceanic and Atmospheric Administration/Geophysical Fluid Dynamics Laboratory Tropical Cyclone tracker analysis tool (TCtracker; Vitart and Stockdale, 2001) are open-source tools. The former was developed for tracking ECs and the other for TCs, although Stormtracks can only read input data from the C20 Reanalysis Project. In addition, while TempestExtremes and Obuko-Weiss-Zeta (OWZ; Tory et al., 2013b) are open-source codes and easily parallelizable using MPI, TRACK is a non-open source, its parallelization is limited on a year to year basis (Bourdin et al., 2022), and it needs to run globally due to the application of spectral filtering during the critical stage of cyclone centres detection. Similarly, the tracker from the Centre National de Recherches Météorologiques (CNRM, Chauvin et al., 2006) is another non-open access code which does not have any parallelization implemented (Bourdin et al., 2022). Likewise, CycloTRACK is non-open access, although it can be obtained from the corresponding author upon request.

The output information provided to the user is also a point for improvement as quite often these available methods do not provide all the necessary output information to users. In this context, we are confident that a tracker product that includes ample physical diagnostic information about the phenomenon represents a huge benefit compared to publicly available tracking methods, given the inevitable computational and time cost that those methods require in post-processing steps. In fact, previous works have often needed to post-processed tracker outputs, i.e., determining the cyclone three-dimensional thermal structure by applying the cyclone phase space (CPS) proposed by Hart (2003), temperature anomaly or a geopotential thickness, to filter TCs (Roberts et al., 2020), SCs (de Jesus et al., 2022; Gozzo et al., 2014) or tropical-like cyclones (TLCs) in the Mediterranean region (Zhang et al., 2020).

Therefore, this work aims to introduce CyTRACK (Cyclone TRACKing framework), a new open-source, comprehensive and user-friendly Python toolbox for detecting and tracking cyclones in model and reanalysis datasets. The remainder of the paper is organized as follows: Section 2 describes the algorithms and kernel of CyTRACK framework. Datasets and validation methods are presented in Section 3. The performance of CyTRACK for tracking TCs and ECs in the North Atlantic basin (NATL), SCs in South Atlantic Ocean (SATL) and MCs in the Mediterranean region are then provided in Section 4, followed by Conclusions and future improvements in Section 5. The default input parameters for tracking TCs, MCs, ECs and SCs are provided in Supplementary Material.

2. CyTRACK algorithms and kernel

The wide cyclone tracking literature available includes many algorithms to identify cyclone centres and the corresponding trajectories in reanalysis datasets and numerical weather prediction model outputs (see Neu et al., 2013; Ullrich and Zarzycki, 2017; Murata et al., 2019; Flaounas et al., 2023, and references therein). Although the geopotential height at 1000 hPa and the vorticity at 850 hPa have been used to track cyclones, most previous studies employed the mean sea level pressure (MSLP). Therefore, CyTRACK detects and tracks cyclones also using the MSLP. Like most algorithmic Lagrangian trackers, the procedure for detecting cyclones is divided into two parts: (i) critical centres detection and (ii) pairing centres in continuous time steps. These procedures are described below.

2.1. Detecting critical centres

Critical centres are detected as mean sea level pressure (MSLP) minima and must satisfy the following conditions:

i. The MSLP value is lower than a specified MSLP threshold (*min_slp_threshold*).
ii. The MSLP anomaly computed as the difference between the MSLP at time t_0 and the mean MSLP in the previous *N* days (*prev_days*) is lower than a critical value (*mslp_anomaly_threshold*).
iii. The MSLP increases (*dmslp_great_circle_distance*) over a specified distance (*great_circle_distance*) from the candidate point.
iv. The maximum wind speed (*max_wind_speed_threshold*) around the critical centre (*radius_for_msw*) is higher than a predefined value.
v. The surface relative vorticity (*vorticity_threshold*) is greater than a critical threshold.
vi. The mean radial distance to the last closed isobar is higher than a critical value (*critical_outer_radius*). The radial distance to the last closed isobar is computed following the procedure developed by Rudeva and Gulev (2007).
vii. When several centres exist in a critical radial distance (*filter_center_threshold*), the centre that has the lowest MSLP is retained.

Additionally, CyTRACK allows discarding centres positioned over terrain higher than a critical high (*terrain_filter*). It is important to remark that CyTRACK is sufficiently robust and flexible. Therefore, users can choose and change these threshold parameters without code modification.

2.2. Paring cyclone centres in continuous time steps

Storm centres are linked together if they reoccur in the next time step (t=t_0 + dt) within a critical distance (*dist_threshold*) from the previous low-pressure centre detected at time t_0. If there are multiple identified centres within the critical distance, then the point with the lowest MSLP is chosen as the cyclone centre at the second time step. CyTRACK also allows a one-time step gap. If no centre is detected at time t_0+dt, CyTRACK searches for a candidate point at time t_0+2dt. If at least one point is found at t_0+2dt within a radial distance of two times *dist_threshold* from the cyclone centre at time t_0, then the cyclone centre at time t_0+dt is computed as the average latitude and longitude at time t_0 and t_0+2dt. To account for the "natural evolution" of the cyclone trajectory, the angle between the lines formed by the centres at time t_0 and t_0+dt and t_0+dt and t_0+2dt must be less than 10°. If the last condition is satisfied, the algorithm continues searching for the next centre at time t_0+3dt; otherwise, the track ends at time t_0. At this point, CyTRACK evaluates the lifetime (*dt_lifetime*) of the cyclone, the minimum distance travelled (*minimum_distance_travelled*) from genesis to dissipation, the maximum intensity (*intensity_threshold*) in terms of the maximum wind speed along the track. Additionally, if *checking_upper_levels_parameters* is set to "*yes*" in the configuration file, CyTRACK classifies the cyclone core based on the thermal wind and thermal asymmetry according to the CPS.

2.3. Utilities

2.3.1. Estimating cyclone outer radius based on the mean sea level pressure

CyTRACK applies the Rudeva and Gulev (2007) approach to estimate the outer radius of cyclones. This method maps the MSLP field onto a polar coordinate system centred in the cyclone. The number of radial legs and the radial length of those legs depends on the *d_ang* and *rout* parameters in the configuration file. It first searches along each radial leg for the location where the first radial derivative of MSLP computed at a defined radial spatial step (*dr_res*) tends to zero. The MSLP in this location is considered a critical MSLP value for a given radius. It is important to remark that if the previous condition is not satisfied for any radial distance, the first guess radius for that direction was set equal to the *rout* with the MSLP in this location set to the critical value. After that, the lowest critical MSLP value is considered the MSLP of the outermost closed isobar and then interpolated to each radial leg. Finally, the interpolated points mark the cyclone geometry, which area is considered equal to the area of a virtual circumference centred in the cyclone. Then, the radius of that circumference is assumed as an effective measure of the cyclone's outer radius. This approach has been previously applied to estimate the size of TLCs (Coll-Hidalgo et al., 2022a) and ECs (Coll-Hidalgo et al., 2022b; Pérez-Alarcón et al., 2023b).

2.3.2. Estimating cyclone size based on the wind speed

Cyclone size based on the wind speed is defined, following Schenkel et al. (2017), as the radial distance from the cyclone centre at which the azimuthal-mean 10-m azimuthal wind equal to a critical wind speed threshold (*outer_wind_speed_threshold*). Previous studies (Chavas and Emanuel, 2010; Knaff et al., 2014; Chavas et al., 2015; Pérez-Alarcón et al., 2021) have used 2, 4, 6, 8, 10, and 12 m/s as wind speed thresholds to estimate TC size. First, CyTRACK projects the winds vectors onto the cyclone centre polar coordinates used for calculating the cyclone outer radius applying the MSLP approach; second, it computes the azimuthal wind field; third, it extracts the approximate cyclone size at each radial leg; and finally, it averages the cyclone size of all directions.

2.3.3. Cyclone thermal structure

As mentioned earlier, after CyTRACK determines the pathway of the cyclones, if the *checking_upper_levels_parameters* parameter is set to "*yes*" in the configuration file, it applies the CPS from Hart (2003) to classify the cyclone according to its thermal structure at each track position. The CPS provides three parameters: thermal symmetry of cyclone thickness (B), low-level thermal wind (-VTL) and upper-level thermal wind (-VTU). Parameter B informs about cyclone thermal symmetry, while -VTL and -VTU provide information on whether the cyclone has an associated cold or warm core. According to Hart (2003), $|B| = 10$ m is a convenient threshold for distinguishing frontal from non-frontal structures. Meanwhile, for warm-core (cold-core) cyclones, -VTL and -VTU are positive (negative). Therefore, based on the CPS, CyTRACK classifies the core of the cyclone following Table 1.

Hart (2003) noted that a linear regression fit to the vertical profile of changes in geopotential high (ΔZ) favours an unambiguous magnitude and sign of -VTU and -VTL. Therefore, CyTRACK allows the estimation of these magnitudes using a vertical increment of 50 hPa to more accurately calculate the vertical profile of ΔZ, in agreement with Hart (2003), by setting the *vtl_vtu_lr* parameter in the configuration file equal to "*yes*". Otherwise, -VTU and -VTL will be estimated using the geopotential high at the bottom and top of the tropospheric layers 900–600 hPa and 600–300 hPa. Additionally, if the users aim to filter cyclones by type (i.e., TC, EC, MC, TLC, SC) using the CPS, they must define the -VTU (*VTU_threshold*), -VTL (*VTL_threshold*) and B (*Bhart_threshold*) thresholds in the configuration file. Likewise, they must provide the number of time steps (*core_criteria_length*) in which the cyclone satisfies these critical values.

2.4. Description of CyTRACK input parameters

Table 2 provides a brief description of specific parameters of CyTRACK for tracking cyclones. It is worth noting that the default

Table 1
Classification of cyclone core according to the cyclone phase space (CPS) proposed by Hart (2003).

|B|	-VTL	-VTU	Cyclone Core
<10	>0	>0	Symmetric deep warm core (SDWC)
<10	<0	<0	Symmetric deep col core (SDCC)
<10	>0	>0	Symmetric low warm core (SLWC)
<10	<0	>0	Symmetric low cold core (SLCC)
>10	>0	>0	Asymmetric deep warm core (ADWC)
>10	<0	<0	Asymmetric deep cold core (ADCC)
>10	>0	>0	Asymmetric low warm core (ALWC)
>10	<0	>0	Asymmetric low cold core (ALCC)

Table 2
Description of specific parameters of CyTRACK for tracking cyclones.

Input parameter	Description
checking_upper_levels_parameters	To evaluate or not the cyclone thermal structure using the CPS
vtl_vtu_lr	To compute -VTL and -VTU using a linear regression
max_dist	Radial distance (km) from the cyclone centre to compute the CPS parameters
dt_h	Temporal resolution of input data
max_wind_speed_threshold	Maximum wind speed (m/s) within a critical distance from the cyclone centre
radius_for_msw	Radial distance (km) to compute maximum wind speed around the critical cyclone centre
outer_wind_speed_threshold	Wind speed (m/s) to compute the cyclone size (see Section 2.3.2)
filter_center_threshold	Minimum distance (km) between two critical centres
critical_outer_radius	Minimum radial distance (km) to the outermost closed isobar
rout	External search radius (km) to compute cyclone size
dr_res	Spatial resolution (km) to compute the first radial derivative of MSLP
d_ang	Angular resolution (degrees) to construct the polar coordinates centred in the cyclone centre to compute the cyclone size
terrain_filter	Critical value (m) to discard centres over high terrain
vorticity_threshold	Surface relative vorticity (1/s) threshold
min_slp_threshold	Maximum value of MSLP (hPa) to consider a grid point as a critical centre
dist_threshold	Maximum distance (km) between centres in continuous time steps
great_circle_distance	Radial distance (degrees) for checking the MSLP increase
dmslp_great_circle_distance	Minimum increase of MSLP (Pa) from the cyclone centre to the *great circle distance*
prev_days	Number of previous days (days) to compute the MSLP anomaly
mslp_anomaly_threshold	Mean sea level pressure anomaly (hPa) threshold
intensity_threshold	Maximum intensity (m/s) along the cyclone track
dt_lifetime	Minimum lifetime (hours) of cyclones tracks
minimum_distance_travelled	Minimum distance travelled (km) by the cyclone
VTL_threshold	-VTL threshold to classify cyclone according to the CPS
VTU_threshold	-VTU threshold to classify cyclone according to the CPS
Bhart_threshold	B threshold to classify cyclone according to the CPS
core_criteria_length	Number of time steps (no necessary consecutive) in which the cyclone satisfies the CPS criteria

threshold values used in CyTRACK were mostly obtained from the literature review. Supplementary Tables S1–S5 show these default parameters and the corresponding reference in the literature. In addition, users should read CyTRACK documentation in the GitHub repository for details on the default threshold parameters for tracking ECs, TCs, MCs and SCs. Nonetheless, for more specific studies, we recommend that users perform a sensitive analysis of CyTRACK to threshold parameters.

2.5. Input data

CyTRACK can detect and track cyclones in the European Centre for Medium-Range Weather Forecasts (ECMWF) reanalysis datasets. In particular, if the ERA5 reanalysis (Hersbach et al., 2020) is used as input data and missing files are found during the checking input files step, it automatically downloads them from the Copernicus Climate Data Store (CDS). It is worth noting that the successful download of files depends on the user's configuration to use the CDS Application Program Interface (*cdsapi* Python package). It also can process input data from the Weather and Research Forecasting (WRF) model simulations. Likewise, it can read data from other sources such as several climate and weather datasets.

2.6. CyTRACK outputs

CyTRACK output has a comma-delimited text format following a similar structure to the HURDAT2 (Landsea and Franklin, 2013) dataset provided by the US National Hurricane Center for TCs. Below we illustrate an example of the CyTRACK output.

CyAL00012005, 41,
20051018, 00, 15.75, -80.00, 998.378, 52.92, 483.005, 1006.91, 509.687, SDWC, 50, 32, -4.0,
20051018, 06, 16.0, -80.25, 998.481, 57.49, 558.127, 1009.12, 726.721, SDWC, 70, 21, -1.0,
20051018, 12, 16.5, -80.50, 995.320, 65.33, 453.859, 1008.70, 658.487, SDWC, 72, 58, -2.0,

The CyTRACK output file contains two types of lines, the first is the heading, and the second type informs about the cyclone along its track. The first type has the following format:

CyAL00012005, 41,

The first two characters ("Cy") correspond to CyTRACK identification, and characters 3–4 inform about the search region (**AL**: North Atlantic Ocean for tracking TCs, **NA**: North Atlantic for tracking ECs, **MS**: Mediterranean Sea, **SA**: South Atlantic Ocean). It is important to remark that the search region identifier depends on the *search_region* parameter in the configuration file. Characters after the search region identifier (and before the last four characters) indicate the automated cyclone number ("0001") during the tracking period, while the last four characters show the genesis year ("2005"). Likewise, the characters after the first comma ("41") refer to the cyclone entry number in the database. The rest of the lines contain the data information for each cyclone using the following format:

20051018, 00, 15.75, -80.0, 998.378, 52.92, 483.005, 1006.91, 509.687, SDWC, 50, 32, -4.0,

The first column represents the date in the YYYYMMDD ("20051018") format, while the second column shows the UTC hour of the entry in the HH ("00") format. The third and fourth columns provide the latitude ("15.75") and longitude ("-80.0") of the centre. Latitude (longitude) is negative when the cyclone is in the southern (western) hemisphere. The fifth and sixth columns inform about the minimum central pressure in the centre in hPa ("998.378") and the maximum surface wind speed in km/h ("52.92"). The size of the cyclone in km ("483.005") estimated based on the wind speed (Section 2.3.2) is shown in seventh column, while columns eight and nine give the MSLP in hPa ("1006.91") of the outermost closed isobar and the size of the cyclone in km ("509.687") computed using the MSLP field (Section 2.3.1). Column 10 shows the cyclone core type (SDWC) according to the description displayed in Table 1. Meanwhile, columns 11, 12 and 13 provide the -VTU ("50"), -VTL ("32") and B ("-4.0") parameters of the CPS. Missing values and undefined core type are given by −99999 and UDCC, respectively.

2.7. Parallelization considerations

CyTRACK fits well into a general framework known as MapReduce (Dean and Ghemawat, 2008). As such, it implements a simple parallelization strategy via MPI to detect critical cyclone centres in individual time steps in the Map() part. Meanwhile, it connects candidate points across time to construct cyclone tracks in the Reduce() part. Supplementary Table S6 provides an overview of the computational demands/processing time for one year of simulations for CyTRACK tracking TCs and ECs in the NATL basin, SC in SATL and MCs and TLCs in the Mediterranean region using the 6-hourly ERA5 reanalysis data on a $0.25^\circ \times 0.25^\circ$ horizontal resolution as input. These experiments were performed

on the Finis Terrae III cluster at the Galician Supercomputing Centre (CESGA, Spanish acronym) using 1, 24, 48 and 96 tasks. Overall, computing time ranged from 5 to 7 min (using 96 tasks) to 1.4 h (using one task). However, it notably increases up to 20 min (41 min) for TLCs, 33 min (54 min) for SCs, 2 h (2.5 h) for TCs, 54 min (1.6 h) for MCs, and 5.4 h (7.3 h) for ECs when CyTRACK applied the CPS using 96 (one) tasks to classify cyclones according to their thermal structure. As the CPS analysis is performed in the Reduce() part, the computing time tends to be less dependent on the number of tasks when CyTRACK uses the parallelization strategy via MPI. Based on these results, we suggest users to use parallel runs of CyTRACK during the Map() part, depending on their computing resources, to gain efficiency in reading and processing the input data. It is also important to remark that computing time depends on the search region area, the horizontal resolution of the input dataset and the number of identified cyclones. Future works on the optimal strategies for CyTRACK parallelization are forthcoming.

3. Datasets and validation method

To validate the ability of CyTRACK to detect and track TCs and ECs in the NATL basin, MCs in the Mediterranean region and SCs in the SATL basin, we used as input data the 6-hourly ERA5 reanalysis at a spatial resolution of 0.25° × 0.25° in latitude and longitude and considering the four different search regions depicted in Fig. 1, for each cyclone type. Overall, the domain extends from 0 to 55°N and 110°W-5°E for TCs (red box), from 25 to 75°N and 115°W-25°E for ECs (black box), from 25 to 50°N and 10°W-40°E for MCs (blue box) and 15–45°S and 10–60°W for SCs (green box). Although the validation task is performed for cyclones in the Atlantic Ocean and Mediterranean Sea due to data availability for comparison, we are confident that the flexibility of CyTRACK allows a good performance in detecting and tracking cyclones in the Indian and Pacific Oceans. For example, the global probability density of extratropical (Supplementary Fig. S1) and tropical cyclone (Supplementary Fig. S2) trajectories for the 2020 and 2018 seasons, respectively, captures the regions with high cyclone activity at a global scale, in agreement with previous works (e.g., Neu et al., 2013; Gramcianinov et al., 2020; Ullrich et al., 2021).

3.1. Validation datasets

According to Flaounas et al. (2023), a critical step for assessing the ability of CDTMs to detect and track cyclones (i.e., ECs, MCs) is the absence of reference datasets for benchmarking. Unlike TCs, which are continuously monitored and recorded in each basin, no historical best-track records based on observations exist for ECs, MCs or SCs. Therefore, we used the available datasets from CDTMs to evaluate the performance of CyTRACK. These databases are briefly described below.

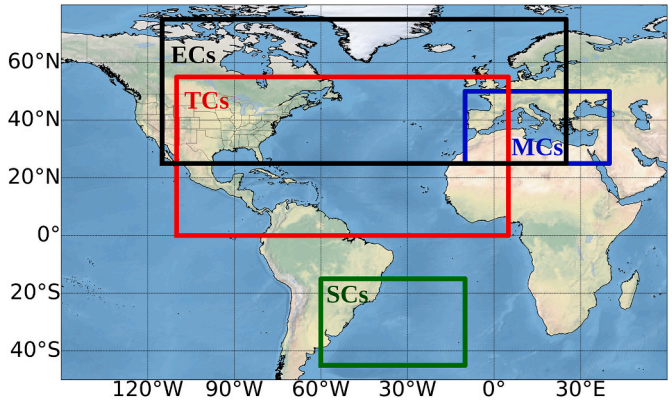

Fig. 1. CyTRACK search region for tracking tropical cyclones (TCs; red box) and extratropical cyclones (ECs; black box) in the North Atlantic Ocean, Mediterranean cyclones (MCs; blue box) in the Mediterranean region and subtropical cyclones (SCs; green box) in the South Atlantic Ocean.

3.1.1. Tropical cyclones

We extracted the best-track records of TCs from the HURDAT2 dataset (Landsea and Franklin, 2013) for TCs, which is known as a high-quality database for the North Atlantic basin. We also compared CyTRACK outputs with TC tracks (without any modification) obtained by Bourdin et al. (2022) using four tracker algorithms fed by the ERA5 reanalysis on a grid spacing of 0.25° and 6 h temporal resolution. Bourdin et al. (2022) applied the UZ kernel implemented in the TempestExtremes framework (Ullrich and Zarzycki, 2017), OWZ, CNRM and TRACK trackers. While UZ and CNRM are based on detecting critical centres in the MSLP field, OWZ evaluates the eponymous Obuko-Weiss-Zeta quantity, and TRACK uses the 850 hPa relative vorticity. For comparison, we used the last ten overlapping years (2009–2018) between all databases to assess CyTRACK performance. Additionally, as we imposed a minimum TC lifetime threshold of 36 h in CyTRACK, we retained from these previous datasets all TCs that existed for at least 36 h. Likewise, we performed the analysis using those TCs formed from May to November.

3.1.2. Extratropical cyclones

Neu et al. (2013) evaluated 15 different cyclone tracking approaches within the community project Intercomparison of Mid Latitude Storm Diagnostics (IMILAST). These 15 tracking algorithms used the ERA-Interim reanalysis (Dee et al., 2011) from ECMWF at 1.5° × 1.5° horizontal grid spacing and 6 h of temporal resolution as input data. Meanwhile, Gramcianinov et al. (2020) recently applied TRACK to the hourly ERA5 reanalysis data to identify ECs in the North Atlantic basin. To assess CyTRACK for tracking ECs, the analysis was restricted to the following nine available datasets (Table 3), with a common ten overlapping years (2000–2009).

CyTRACK also discards cyclones with a lifetime shorter than 48 h, so we removed all cyclones from the databases with a track length shorter than this lifetime threshold. Also note that, in this work, the search region of CyTRACK for tracking ECs is limited (black box in Fig. 1). Therefore, we only retained cyclones within the CyTRACK search region during at least the first nine time steps.

3.1.3. Mediterranean cyclones

Flaounas et al. (2023) applied ten well-established CDTMS (see Table 4 for references) to hourly ERA5 reanalysis fields with a regular grid spacing of 0.25° × 0.25° in longitude and latitude from 1979 to 2020. By overlapping cyclones pathways, they produced MCs composite tracks using different confidence levels (CLs) within a broader Mediterranean region (20°N-50°N and 20°W-45°E). The CL is defined by the

Table 3
Extratropical cyclones datasets. The database code is the same as in Neu et al. (2013), while G20 is referring to Gramcianinov et al. (2020). MSLP: mean sea level pressure; VORT850: vorticity at 850 hPa, and terrain filtering means that cyclones positioned over terrain higher than terrain high threshold are eliminated.

Database	Variable used	Terrain filtering	References to tracking method
M02	MSLP	>1500 m	Simmonds and Murray (1991).; Pinto et al. (2005)
M07	VORT850	None	Flaounas et al. (2014)
M08	MSLP	None	Trigo (2006)
M09	MSLP	None	Serreze (1995); Wang et al. (2006)
M15	MSLP	>1000 m	Blender et al. (1997); Raible et al. (2008)
M20	MSLP	>1500 m	Wernli and Schwierz (2006)
M21	VORT850	None	Inatsu (2009)
M22	MSLP	None	Bardin and Polonsky (2005); Akperov et al. (2007)
G20	VORT850	None	Hodges (1994, 1995, 1999)

Table 4
Cyclone tracking algorithms applied by Flaounas et al. (2023) to produce composite tracks of Mediterranean cyclones (MCs). MSLP: mean sea level pressure; VORT850: vorticity at 850 hPa, Z1000: geopotential high at 1000 hPa. The asterisk indicates algorithms specifically developed for detecting and tracking MCs.

Database	Variable used	References to tracking method
A01*	Z1000	Aragão and Porcù (2022)
A02*	MSLP	Flaounas et al. (2014) adapted to use MSLP
A03*	MSLP	Ziv et al. (2015)
A04*	MSLP; VORT850	Sanchez-Gomez and Somot (2018)
A05*	MSLP	Ragone et al. (2018)
A06*	MSLP	Picornell et al. (2001); Campins et al. (2006)
A07	VORT850	Hodges (1994, 1995, 1999) following Priestley et al. (2020)
A08*	MSLP	Lionello et al. (2002); Reale and Lionello (2013)
A09	MSLP	Ullrich and Zarzycki (2017); Ullrich et al. (2021)
A10	MSLP	Wernli and Schwierz (2006); Sprenger et al. (2017)

number of CDTMs that captured the same system, i.e., a CL of 5 (CL5) indicates that cyclones were detected by at least five CDTMs, so the CL ranges from 2 to 10. Similarly to Flaounas et al. (2023), CyTRACK discarded tracks lasting less than 24 h to exclude short-lived cyclonic patterns; however, the search region by Flaounas et al. (2023) is slightly larger than in this work. Therefore, to objectively evaluate the ability of CyTRACK to capture MCs, we only considered cyclones from Flaounas et al. (2023) within the blue box in Fig. 1. Likewise, we focused on the last ten years with data availability (2011–2020)

3.1.4. Subtropical cyclones

To the best of our knowledge, there are no public datasets of SCs in the SATL basin. Therefore, to assess the performance of CyTRACK in detecting and tracking SCs in SATL, we compared CyTRACK outputs from 2006 to 2015 with previous climatologies (e.g. Gozzo et al., 2017; de Jesus et al., 2022). Additionally, as an example, we extracted from Reboita et al. (2019) the pathways of three SC formed on the southeastern Brazilian coast and compared them with the corresponding tracks in CyTRACK. Reboita et al. (2019) tracked these storms using the relative vorticity at 925 hPa from ERA5 reanalysis.

3.2. Cyclone track-to-track comparison

When CTDMs are applied to reanalysis or modelling datasets, identified tracks can be associated with observed or reference tracks (Murakami, 2014; Hodges et al., 2017; Ullrich et al., 2021; Bourdin et al., 2022). In this work, we evaluated the correspondence between individual cyclone tracks in CyTRACK with pathways in the benchmarking datasets by applying the track-to-track comparison method proposed by Hodges et al. (2003). We first identified track points in CyTRACK that overlap in time with track points in the reference dataset. If the number of overlapping points is equal to or higher than 60% of the mean number of points between the two tracks, a matching in time is found. Then, if the mean distance between the overlapping points is less than 300 km, a pair of matching tracks is detected. It is important to remark that more than one track in CyTRACK can satisfy the temporal matching threshold. Therefore, the one with the lowest mean distance from the reference track is considered a matching track. Previous studies (e.g. Xia et al., 2012; Di Luca et al., 2014; Bourdin et al., 2022; Dulac et al., 2024; Flaounas et al., 2023) have used 300 km as a threshold for the mean separation between overlapping points.

After the matching track procedure is completed, we computed the track agreement as the percentage between matching tracks and the lower number of tracks between CyTRACK and the benchmarking dataset. For the case of TCs, as we applied the track-to-track comparison method to the best-track database (HURDAT2), we also computed the false alarm rate (FAR) as the relationship between False Alarms and the sum of matching and missing tracks.

4. Results and discussion

4.1. Tropical cyclones

Fig. 2 shows the annual (from 2009 to 2018) and monthly frequency of TCs in the NATL basin, as well as the track duration and the track agreement between CyTRACK and the benchmarking datasets. Overall, the annual (Fig. 2a) and monthly (Fig. 2b) TC number detected by CyTRACK agree particularly well with the temporal distribution from the HURDAT2 dataset. However, although CyTRACK exhibits an annual and seasonal evolution similar to TRACK, CNRM, UZ and OWZ, it is characterized, similarly to HARDUT2, by a higher number of detected TCs. This behaviour could be related to the post-treatment method by Bourdin et al. (2022) to filter TCs from the total number of cyclone tracks yielded by the four trackers.

The average lifetime of TCs detected with CyTRACK (~7.4 days) is similar to the observed in HURDAT2 (~7.6 days) and UZ (~7.7 days) but lower than CNRM (~8.0 days), OWZ (~11.1 days) and TRACK (~13.2 days). Indeed, substantial differences in the distribution of track duration can be observed among methods (Fig. 2c), with peaks at ~5 days for CyTRACK, HURDAT2, UZ and CNRM, and significantly longer it peaks at 9 and 12 days for OWZ and TRACK. Previously, Bourdin et al. (2022) found that the peak of track duration distributions for UZ, CNRM, OWZ, and TRACK were 5, 6, 8, and 12 days, respectively, but including all basins with TC activity. Hodges et al. (2017) documented longer track duration using TRACK fed by other reanalysis datasets. In particular, tracking methods based on relative vorticity tend to capture longer cyclone tracks as they are more capable of identifying and tracking small-scale features (Hoskins and Hodges, 2002; Neu et al., 2013; Hodges et al., 2017; Grieger et al., 2018), such as precursor stages (e.g. wave disturbances) or persistent disturbances after landfall (Bié and de Camargo, 2023).

Fig. 2d displays the track agreement between CyTRACK and benchmarking datasets. CyTRACK detected ~73–79% of TCs in the reference databases. In particular, the track agreement between CyTRACK and HURDAT2 accounts for ~74%. Bourdin et al. (2022) found that UZ, CNRM, TRACK and OWZ matched, respectively, 58% (74%), 62% (74%), 63% (84%), 67% (76%) of observed TCs in the NATL (global) basin from 1979 to 2019. Meanwhile, Ullrich et al. (2021), applying the TempestExtremes, found a global hit rate of 78%. Recently, Dulac et al. (2024) assessed the representation of TCs in ERA5 reanalysis with the CNRM tracker and found a track agreement of ~57%. Likewise, the FAR of CyTRACK is about 25%, which is lower (higher) than that found by Bourdin et al. (2022) for TRACK and CNRM (UZ and OWZ) for the NATL basin. As CyTRACK tracked all TC categories, the track agreement with HURDAT2 is highly biased by weaker storms and perturbations observed and included in HURDAT2, which are not strong enough to exceed the detection thresholds criteria, in agreement with Hodges et al. (2017) and Bourdin et al. (2022). At this point, it is important to note that track agreement and FAR differences between CyTRACK and previous works using other trackers can also be influenced by the track-to-track comparison method. Nonetheless, these results suggest that CyTRACK shows similar skills to other trackers to detect and track TCs.

Further insight into the analysis of TCs frequencies is obtained by examining the spatial distribution of cyclone track density. The spatial distribution of TC tracks has critical importance due to the regionalized nature of TC impacts (Vecchi et al., 2014). Fig. 3 shows that the patterns of TC track density, especially local maxima, are comparable between the trackers and HURDAT2. Indeed, it is clear all trackers yield reasonable distributions of TC occurrence when compared to HURDAT2 (Fig. 3e), although subtle differences appear upon closer analysis. Overall, the four trackers, in agreement with HURDAT2, highlight the tropical NATL region spanning from the western African coast to the

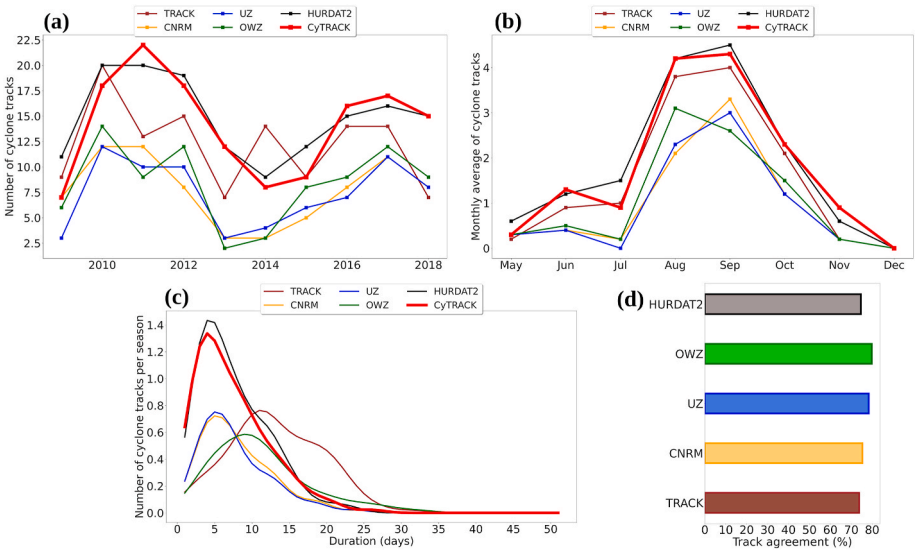

Fig. 2. **(a)** Annual and **(b)** monthly frequency of TCs in the North Atlantic basin, **(c)** distribution of the duration of TCs and **(d)** track agreement (%) between CyTRACK and benchmarking datasets. The analysis period ranges from 2009 to 2018.

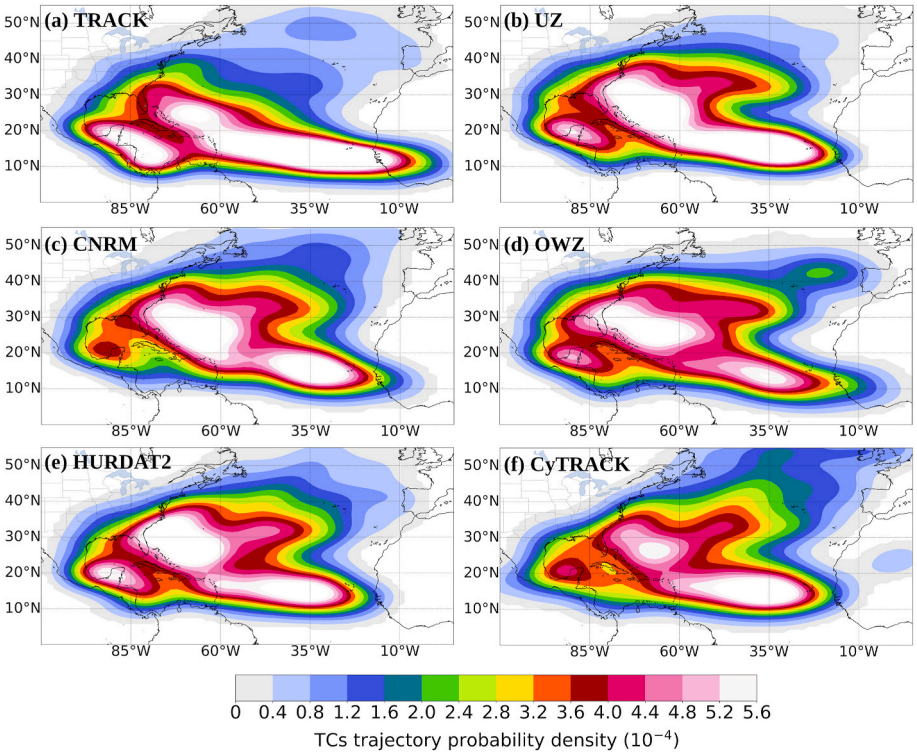

Fig. 3. Probability density of tropical cyclones trajectories from **(a)** TRACK, **(b)** CNRM, **(c)** UZ, **(d)** OWZ, **(e)** HURDAT2 and **(f)** CyTRACK.

Lesser Antilles Arc, the western NATL northeastern of the Bahamas Archipelago and the Gulf of Mexico as the most TC active areas in the NATL basin. However, TRACK detected a high track density extending from the Gulf of Mexico to the Caribbean Sea and missed the secondary maximum of TC tracks, observed in all other datasets, oriented eastward towards the Azores. The UZ tracker merged the tropical and western NATL in a wider local maximum. The differences in the spatial distribution of the track density can be related with differences in TC lifetimes (Fig. 2c). Nonetheless, we also found highly statistically significant scores by computing the Pearson correlation between CyTRACK and benchmarking datasets. The correlation coefficient ranged from 0.82 to 0.96, with the lowest achieved by comparing with TRACK and the highest with HURDAT2. A previous study by Zarzycki et al. (2021) found similar Pearson correlation coefficients by comparing TempestExtremes applied to different reanalyses with observations.

We also investigated the ability of CyTRACK to reproduce the wind-pressure relationship detected by the four trackers (Fig. 4). This relationship is often used in studies of TCs to assess the ability of models and reanalyses to represent the intensity of TCs by comparing it with the observed relationship (Roberts et al., 2015; Hodges et al., 2017). Overall, both CyTRACK and the four trackers tend to reproduce TCs with less intense maximum wind speed concerning their central pressure, in agreement with previous studies (Hodges et al., 2017; Bell et al., 2018; Bourdin et al., 2022; Bié and de Camargo, 2023). This mismatch reflects

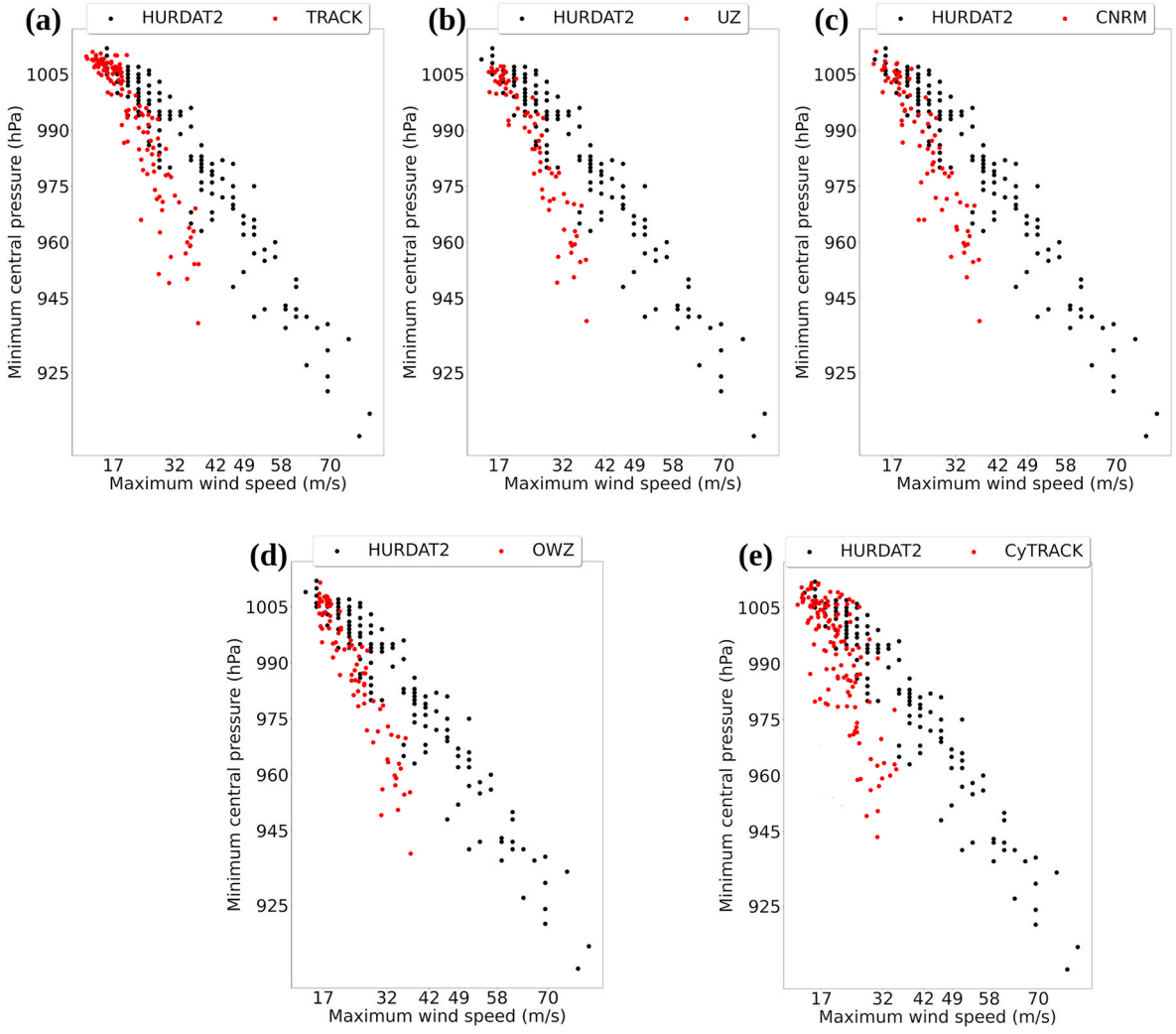

Fig. 4. Wind–pressure relationships for **(a)** TRACK, **(b)** UZ, **(c)** CNRM, **(d)** OWZ, and **(e)** CyTRACK compared against the HURDAT2 dataset. The x-axis and y-axis ticks show the TC intensity category boundaries based on the Saffir-Simpson wind scale and Klotzbach et al. (2020), respectively.

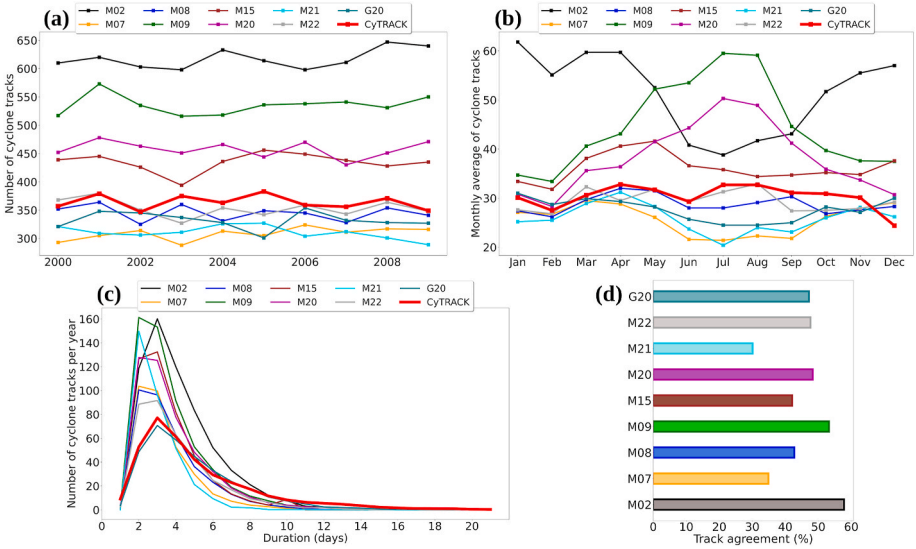

Fig. 5. **(a)** Annual and **(b)** monthly frequency of ECs in the North Atlantic basin, **(c)** distribution of the duration of ECs and **(d)** track agreement (%) between CyTRACK and bencmarking datasets. The analysis period ranges from 2000 to 2009.

the underestimation of the intensity of TCs, particularly for the most intense systems.

4.2. Extratropical cyclones

Neu et al. (2013) shows that CTDMs produce a wide range of results for EC frequency in the Northern and Southern Hemispheres. Consistent with these hemispheric results, the total count of ECs in the NATL basin from 2000 to 2009 exhibits a large difference between tracking methods, as shown in Fig. 5a. In terms of annual frequency, CyTRACK yields ~354.9 ± 14 (one standard deviation) ECs per year, being quite similar to M22 (353.5 ± 14), M08 (344.9 ± 12) and G20 (332.1 ± 14). Meanwhile, M02 (617.4 ± 16) and M09 (535.5 ± 16) detected the largest number of tracks and M21 (310.6 ± 11) the lowest. It is worth noting here that CyTRACK, M22 and M08 are based on MSLP, while G20 is based on relative vorticity at 850 hPa (VORT850). Similarly, M21 and M09 produce EC tracks based on MSLP, and M21 on VORT850. These significant differences confirm that the annual count of ECs depends more on the threshold criteria used in the tracking method than on the variable used, in agreement with Grieger et al. (2018).

The monthly frequency of ECs shows a wide range of annual cycle behaviour. Thus while M02 presents the highest number of tracks in winter months, M09 and M20 peak in summer (Fig. 5b). Meanwhile, the remaining trackers, including CyTRACK, exhibit a lesser marked seasonal variability. Again, CyTRACK performs similar to M08 and M22. Despite differences in the annual and seasonal frequencies, the average ECs lifetime ranged from 3.1 to 5.0 days. The M21 (~3.1 days) and M07 (~3.5 days) produce the most short-living cyclones, while G20 (~4.9 days) and CyTRACK (~5.0 days) produce the long-living ECs. Previously Neu et al. (2013) highlighted the tendency of M21 to produce short-living cyclones, while Gramcianinov et al. (2020) estimated a mean lifetime of 4.4 days of ECs in NATL from 1979 to 2019. By comparing the distribution of the track duration of ECs per year, M09 and M21 peak at 2 days, while most of the remaining trackers peak on 3.5 days. Interestingly, although G20 and CyTRACK detect and track cyclones using different approaches, they exhibit a similar distribution in the cyclone tracks per year.

The track-to-track comparison method between CyTRACK and the benchmarking datasets shown in Fig. 5d reveals an overall track agreement ranging from 30% to 57%. Contrary to what we can expect from the previous analysis, the lowest track agreement was detected by comparing CyTRACK with M21. The highest agreement of CyTRACK was achieved with M02 (57%) and M09 (53.8%), while also matched 47.2% of tracks in G20. Similar track agreements were found by Wang et al. (2016) by comparing the cyclone tracks produced by an improved version of M09 (Wang et al., 2013) using different reanalysis datasets. Likewise, the track agreement between methods in Neu et al. (2013) ranged from roughly 50%–70%. According to Neu et al. (2013), differences between trackers are more likely a consequence of different approaches, use of MSLP vs. vorticity, threshold parameters and thresholds criteria applied to those parameters. From Fig. 5, the best match was generally with trackers that produced the highest number of cyclones, as in M02 and M09.

We also compared the trajectory densities from all trackers from 2000 to 2009. Although CyTRACK exhibits a lesser intense track density, Fig. 6 shows an overall agreement between methods in terms of NATL

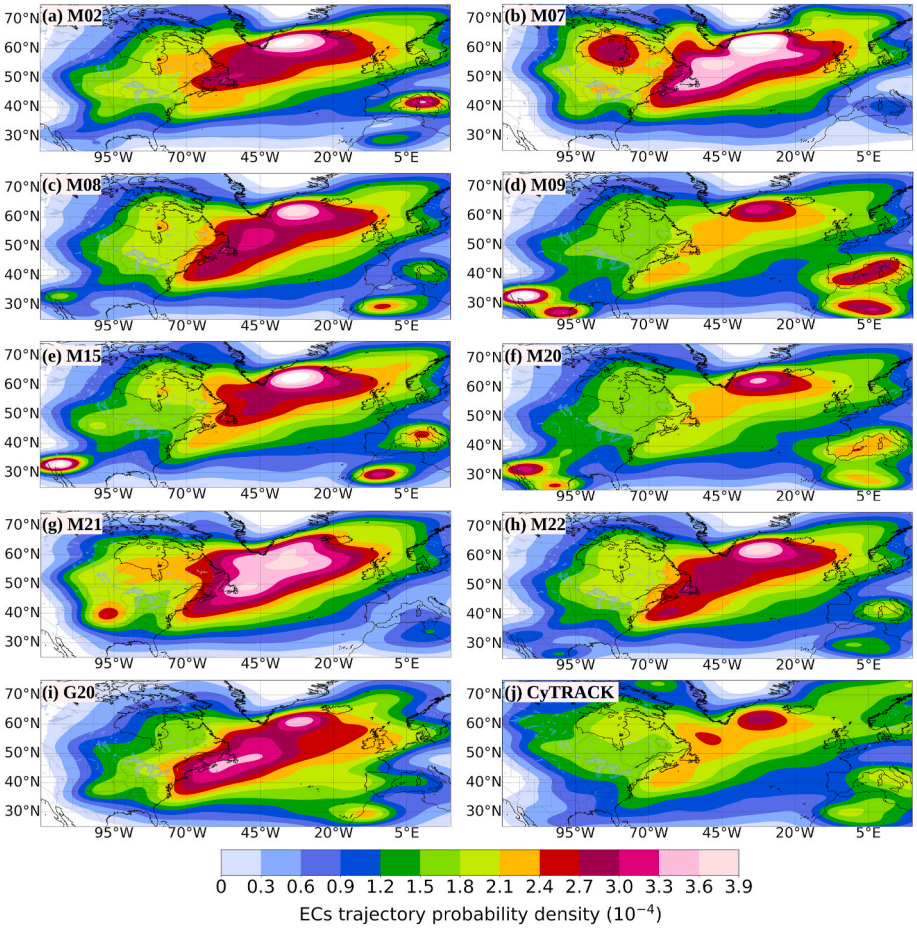

Fig. 6. Probability density of extratropical cyclones trajectories from **(a)** M02, **(b)** M07, **(c)** M08, **(d)** M09, **(e)** M15, **(f)** M20, **(g)** M21, **(h)** M22, **(i)** G20 and **(j)** CyTRACK.

storm track, extending northeastward from the eastern North American coast to Greenland and North Europe. There are, in contrast, noteworthy differences in the Mediterranean region attributed to threshold criteria and the small size of Mediterranean cyclones. Note that the track density presented here is not directly comparable to the track frequencies shown in Fig. 5 because each track consists of a different track duration, in agreement with Grieger et al. (2018). The Pearson correlation scores reflect the differences in the track density patterns. Although visually, the track density from CyTRACK is quite similar to M09 and M20, the highest Pearson correlation coefficients were found for M22 (0.89) and M08 (0.88), suggesting a high agreement between CyTRACK and M22 and M08 in the location of track density maxima. This result supports the previous analysis.

Overall, the differences between CyTRACK and benchmarking datasets can be generally attributed to the variable used for tracking, the threshold criteria (e.g., lifetime, intensity, terrain filtering), and the horizontal and temporal resolution of the data used. While all methods from Neu et al. (2013) used 6-hourly ERA-Interim, G20 used hourly ERA5 and CyTRACK 6-hourly ERA5.

4.3. Mediterranean cyclones

Based on the composite tracks from Flaounas et al. (2023), we assessed the ability of CyTRACK to identify and track MCs. Fig. 7a shows the annual number of MC tracks from CyTRACK and reference datasets. In this case, the differences in track counts are attributed to the gradual decrease of MC numbers with confidence level increases, in agreement with Flaounas et al. (2023). On average, the annual number of cyclones from CTDMs in Flaounas et al. (2023) varied from 100 to 120 (A04, A08, A10) to 500 (A03), and the composite tracks ranged from 4 in the confidence level 10 (CL10; the number of CDTMs that captured the same system) to 171 in CL2. Meanwhile, CyTRACK produces 184 ± 8 tracks per year.

The monthly distributions of MC frequency mostly peak in April and May (Fig. 7b, except for CL2 and CL3). Previous works detected a similar seasonal variability (e.g. Campins et al., 2011; Lionello et al., 2016; Kotsias et al., 2023). For example, Kotsias et al. (2023), by applying A08 to ERA5 reanalysis, attributed the high frequency of MC in April to cyclone activity over the land due to the intense land warming and the upper air disturbances. Nonetheless, Flaounas et al. (2023) noted that CTDMs agree on the seasonal cycle of well-developed intense MCs than on shallow MCs. Overall. CyTRACK tends to capture well the monthly distribution of MCs considering that the most intense MCs often occur in winter and spring (Flaounas et al., 2015, 2022) and the direct linkage between MC seasonal frequency and intensity (Flaounas et al., 2023).

MCs typically present shorter lifetimes than cyclones that form over open oceans (Flaounas et al., 2014, 2022). The mean lifetime of MCs in the benchmarking datasets increases as a function of the confidence level from 46 h (CL2) to 85 h (CL10). However, according to Flaounas et al. (2023), the lifetimes for the high confidence level datasets are exceptionally long by comparison with tracks from individual CDTMs, which lasted, on average, from 24 to 48 h. The mean MC lifetime from CyTRACK is 44 h. The differences in the MC lasting time are reflected in the distribution of track duration in terms of cyclones per year, shown in Fig. 7c. While the distribution of MC duration from CyTRACK peaks at approximately 30 h, the peak from the composite track datasets increases from 30 to 66 h as the confidence level increases.

Fig. 7d shows the track agreement between CyTRACK and the composite tracks from Flaounas et al. (2023). The track agreement score ranges from 50% (CL2) to 97.5% (CL10). The performance of CyTRACK suggests that it is skillful to capture most of the objectively tracked cyclones using other tracking methods. For example, the composite track of confidence level 2 (CL2) indicates that two CTDMs identified the same MC, and therefore, CyTRACK probably matches at least 50% of individual tracks from individual CTDMs. Indeed, the track-to-track comparison performed by Flaounas et al. (2023) yielded track agreement scores between individual CTDMs ranging from 20 to 67%. Likewise, the increasing tracking scores from low to high confidence levels in the benchmarking datasets was also achieved by Flaounas et al. (2023).

The spatial distributions of MCs track density for CyTRACK and benchmarking datasets from 2 to 6 confidence levels are depicted in Fig. 8. Overall, CyTRACK agrees on the local maxima track density detected by composite tracks with higher densities being located over maritime areas, close to the Gulf of Genoa in the northwest Mediterranean Sea. Other local maxima of track density are also commonly found over northwestern Africa, the Turkish coasts, the Black Sea and the Adriatic and Ionian seas. These areas have been identified in previous studies (Lionello et al., 2016; Flaounas et al., 2018; Reale et al., 2022; Aragão and Porcù, 2022). Flaounas et al. (2023) obtained similar patterns of MC track densities from the ten CTDMs used to generate the composite tracks. These results are reflected by the statistically significant Pearson correlation coefficients between CyTRACK and reference datasets, ranging from 0.74 (CL10) to 0.90 (CL3).

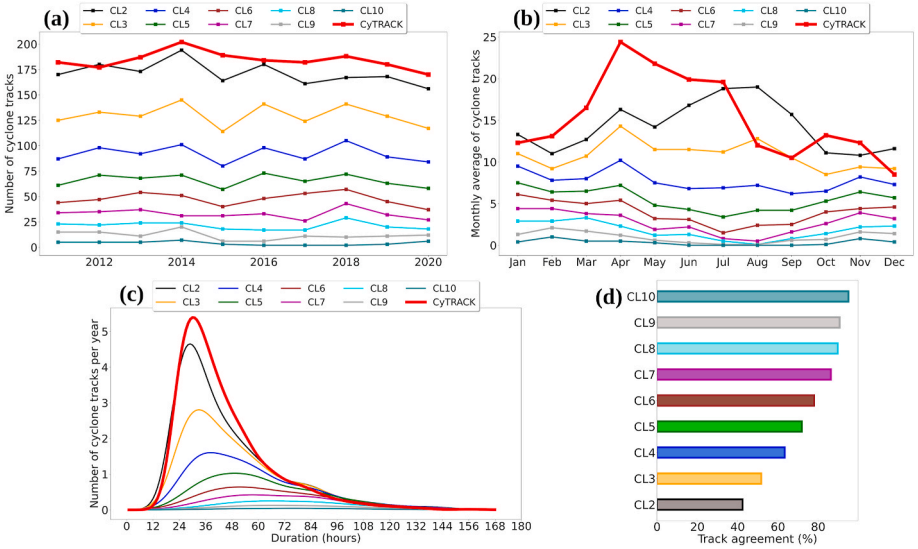

Fig. 7. **(a)** Annual and **(b)** monthly frequency of MCs in the Mediterranean region, **(c)** distribution of the duration of MCs and **(d)** track agreement (%) between CyTRACK and benchmarking datasets. The analysis period ranges from 2011 to 2020.

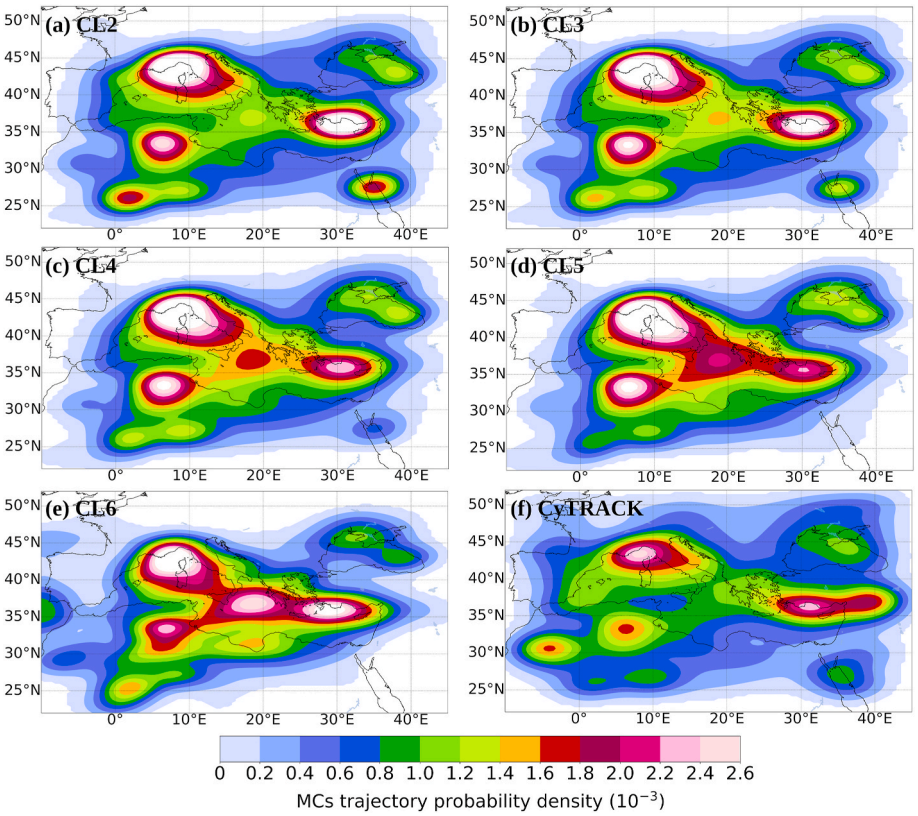

Fig. 8. Probability density of Mediterranean cyclones trajectories from **(a)** CL2, **(b)** CL3, **(c)** CL4, **(d)** CL5, **(e)** CL6 and **(f)** CyTRACK.

4.3.1. The special case of medicanes

The Mediterranean region is also characterised by the development of cyclones that exhibit noticeable similarity to their tropical counterparts for their dynamical and thermodynamic features and for their appearance in satellite images (Miglietta and Rotunno, 2019; Flaounas et al., 2023). These storms are known as TLCs or MEDIterranean hurriCANES (medicanes). TLCs are generally detected using CTDMs if the cyclone shows vertical symmetry and a warm-core structure for more than 10 % of the track or more than 6 h (Cavicchia et al., 2014; Zhang et al., 2020). Here we show the results obtained with CyTRACK when the CPS is applied along the trajectory of all MCs to detect TLCs. During the study period (2011–2020), CyTRACK found ~6.7 ± 1.4 TLC per year distributed throughout the year (Fig. 9a and b). The annual number of TCLs detected here noticeably differs from previous climatologies. For example, Romero and Emanuel (2013) reported 1.5 ± 0.9 TLCs/year, Cavicchia et al. (2014) also found low TLC frequency values of 1.57 ± 1.30 per year, Nastos et al. (2018) found ~1.4 ± 1.3 TLCs/year and Zhang et al. (2020) detected ~1.5 TLCs/year. These differences are

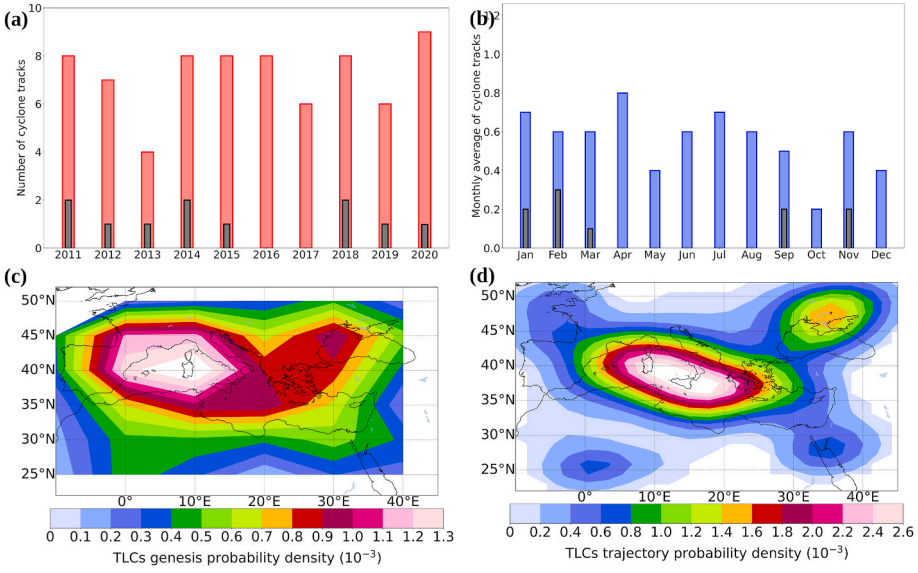

Fig. 9. **(a)** Annual and **(b)** monthly frequency of TLCs in the Mediterranean region. The gray bars denote the TLC activity using the intensity threshold of 17 m/s. **(c)** Probability density of TLC genesis and **(d)** trajectories. Panels (c) and (d) are from the resulting tracks using an intensity threshold of 10 m/s.

attributable to the maximum intensity threshold imposed in these previous works. Indeed, Gaertner et al. (2018) highlighted that TLC identification is sensitive to the intensity threshold criteria. Zhang et al. (2020) varying the threshold criteria for MSLP, maximum wind speed, and warm core detected a climatological frequency of TLCs ranging from 0.9 to 2.9. Similar behaviour occurs in the monthly distribution. While CyTRACK detected TLCs in every month of the calendar, with the highest frequency in January, April and June (Fig. 9b), previous studies (Cavicchia et al., 2014; de la Vara et al., 2021; Zhang et al., 2020) found the highest number of TLCs in winter (from December to February) and no development in summer (from June to August). However, by changing the intensity threshold in CyTRACK from 10 m/s to 17 m/s, the annual frequency of TLCs decreased to 1.1 ± 0.8 cyclones per year, and the winter season achieved the highest TLC frequency, in agreement with the previous studies.

Despite to the differences in the annual and monthly distribution of TLCs, the genesis (Fig. 9c) and trajectory (Fig. 9d) probability densities from CyTRACK agree with previous climatological studies (Romero and Emanuel, 2013; Cavicchia et al., 2014; Tous et al., 2016; Flaounas et al., 2018). Fig. 9c shows that the genesis of TLCs more frequently occurs in the western Mediterranean Sea, followed by the Ionian Sea between Sicily and Greece. Similarly, the highest track densities (Fig. 9d) extend from the western to central Mediterranean Sea.

4.4. Subtropical cyclones

From 2006 to 2015, CyTRACK detected 99 SCs in the South Atlantic ocean domain (green box in Fig. 1), representing an annual value of ~9.9 ± 4.2 SCs per year (Fig. 10a), with the monthly distribution peaking from November to March and notably decreasing from June to August (Fig. 10b). Gozzo et al. (2017) and Cardoso et al. (2022) previously detected 7.2 ± 2.88 SCs per year (using ERA-Interim from 1979 to 2015), and de Jesus et al. (2022) found 8.0 ± 2.5 cyclones per year (using ERA-Interim from 1979 to 2005) with a similar seasonal frequency. Our analysis also shows that the mean lifetime of SC is approximately 4.2 days, and its distribution peaks at ~3 days (Fig. 10c), in agreement with Gozzo et al. (2014) and de Jesus et al. (2022).

Furthermore, regarding the genesis area, CyTRACK and previous climatologies (Gozzo et al., 2014, 2017; de Jesus et al., 2022) present a similar spatial pattern of mean subtropical cyclogenesis density (Fig. 10d), with the main development region close to the southeastern coast of Brazil. Nevertheless, in terms of the track density, while these previous studies found the core close to the Brazilian coast, the trajectories from CyTRACK exhibit the peak of track density southeastward shifted (Fig. 10e). Overall, the differences between CyTRACK and these previous climatologies can be mostly attributed to the fact that some SCs in the searching region do not exhibit a closed contour pattern in the MSLP field (Gozzo et al., 2014), and the intensity threshold based on 10m wind speed and MSLP used in CyTRACK.

In order to provide an example of the ability of CyTRACK to detect and track SCs, Fig. 11 displays the trajectories of three named SCs extracted from Reboita et al. (2019) and CyTRACK. Note that, despite the slight separation between the tracks, there is an overall agreement in the genesis regions and pathways. Again, the differences are attributable to differences in tracking methods. While CyTRACK tracked this storm using the MSLP field, Reboita et al. (2019) used the relative vorticity in 925-hPa.

5. Conclusions

Automated cyclone detection and tracking methods (CDTMs) have been widely applied to detect and track cyclones in reanalysis and

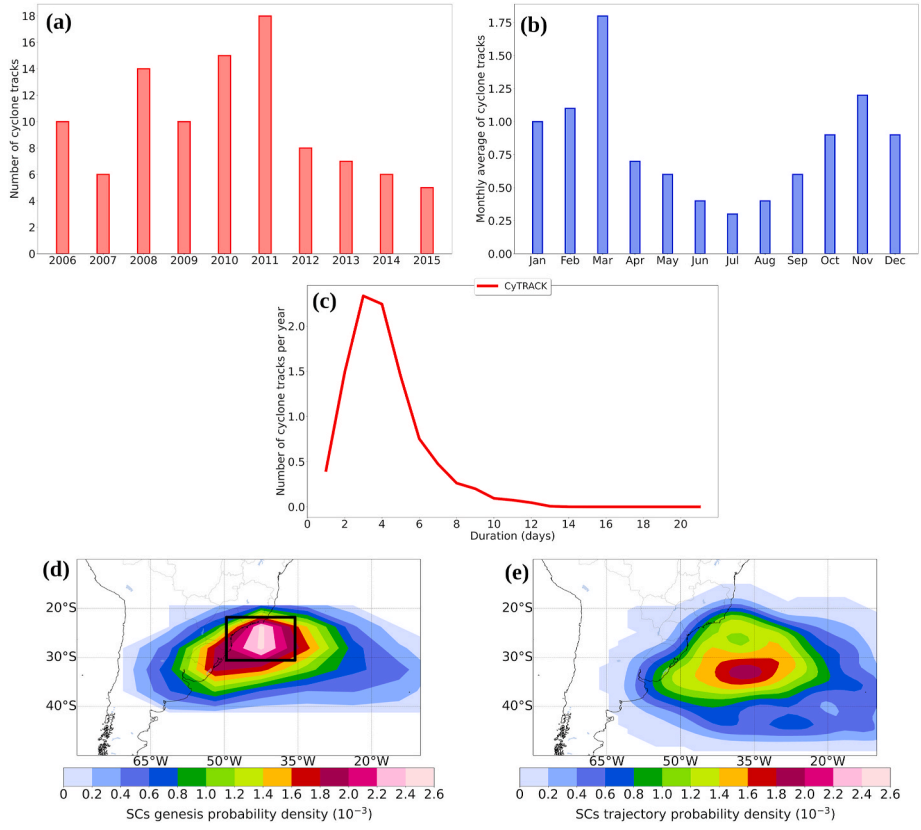

Fig. 10. **(a)** Annual and **(b)** monthly frequency of SCs in the South Atlantic Ocean. **(c)** distribution of the duration of SCs. **(d)** Probability density of SC genesis and **(e)** trajectories. The black box in panel (d) represents the main cyclogenesis region (30.58–21.8°S and 49.58–35.58°W) of SCs in the South Atlantic Ocean found by Gozzo et al. (2014). The analysis period ranges from 2006 to 2015.

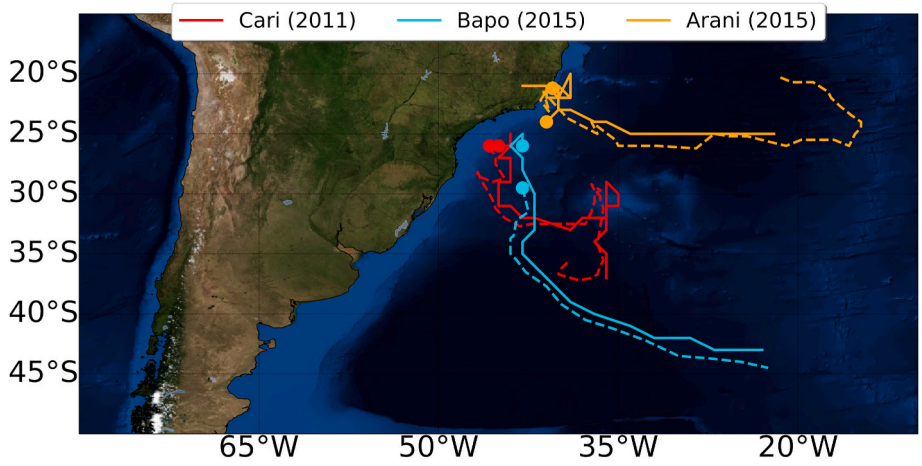

Fig. 11. Trajectories of three SCs named Cari (2011), Bapo (2015) and Arani (2015) extracted from Reboita et al. (2019) (solid lines) and CyTRACK (dashed lines). The marker denotes the genesis location.

modelling datasets. CDTMs are an important tool for extracting relevant information on cyclone activity from climate models to understand how global warming will impact genesis locations, storm tracks, and intensity of future cyclones. This work outlined CyTRACK (Cyclone TRACKing framework), a new open-source, comprehensive and user-friendly Python toolbox for detecting and tracking cyclones in reanalysis and observational datasets and climate model simulations, exposing the characteristics of the detection and tracking algorithm and the suite of input parameters. CyTRACK is sufficiently flexible and robust, allowing users to change the threshold criteria without code modifications and also by classifying cyclones based on their thermal structure during the tracking and pairing centres steps. Additionally, it is useful for computing optimal threshold values for detecting pointwise features in different temporal and spatial resolution datasets and also for sensitive studies to test the threshold values of the CPS for classifying cyclones.

The evaluation of CyTRACK outputs for ten years against best-track archives and available datasets from other tracking algorithms showed its ability to detect and track cyclones. Nonetheless, the evaluation presented here was not global but focused on tropical and extratropical cyclones in four specific domains including the North Atlantic basin, Mediterranean cyclones and subtropical cyclones in the South Atlantic Ocean. In general, differences between databases are noticeable concerning the overall number of cyclones, in particular, influenced by the tracks of weak cyclones. However, there is a substantial agreement on the annual and monthly variability of cyclone frequency, life cycle characteristics and spatial distribution of track densities. Our analysis also confirms that different CDTMs applied to the same dataset or a single CDTM applied to several datasets produce slightly different results.

It is well-known that CDTMs follow different understandings of the cyclone features, and choosing a particular tool should follow the study goals. Although CyTRACK is easily adaptable to specific user objectives through flexibility in modifying critical parameters in the configuration file, it has some limitations. Detecting and tracking cyclones in CyTRACK depends on the correct choice of threshold parameters, which should represent the characteristics of the cyclones under study. In particular, one should note that the use of more restrictive parameters tends to eliminate weak systems, while opting for more relaxed ones may lead to increasing false alarms. In addition, validating CDTMs is problematic because, except for TCs, there is no universally agreed set of historical storm tracks for comparison. Likewise, the limitations of the reanalyses in resolving cyclone scale processes and representing the cyclone surrounding environment is another source of uncertainties.

We acknowledge that even when CyTRACK appears successful in detecting and tracking cyclones, there will always be scope for further improvement. On this basis, the ongoing development of CyTRACK includes other widely used meteorological fields to detect critical cyclone centres, such as relative vorticity. Future works will also focus on improving the parallelization strategies to reduce the computing time. Likewise, we will continue to work on maximizing the robustness of CyTRACK across all data sets to ensure it is useful for comparative analyses across models, multi-model ensembles and reanalysis products. CyTRACK is implemented in Python, and its source code is freely available from the GitHub repository at https://github.com/apalarcon/CyTRACK.

Software and data availability

Software name: CyTRACK
Developer: Albenis Pérez-Alarcón, Co-developers: Patricia Coll-Hidalgo, Ricardo M. Trigo, Raquel Nieto, and Luis Gimeno
Contact information: albenis.perez.alarcon@uvigo.es
Year first available: 2024
Hardware requirements: PC, HPC
System requirements: Linux, Windows
Program language: Python
Program size: 2.5 MB
Availability: https://github.com/apalarcon/CyTRACK
License: GNU Public License (GPLv3)
Documentation: README in the Github repository.
Data Availability: ERA5 data are available on the Copernicus Climate Change Service Climate Data Store (CDS, https://cds.climate.copernicus.eu/. This work also uses several datasets to evaluate the ability of CyTRACK to detect and track cyclones in the North and South Atlantic Ocean and the Mediterranean region. The HURDAT2 database can be obtained from https://www.nhc.noaa.gov/data/hurdat/hurdat2-1851-2022-050423.txt. The UZ, OWZ, CNRM and TRACK outputs from Bourdin et al. (2022) are available at https://doi.org/10.5281/zenodo.6424432. The CTDMs outputs from Neu et al. (2013) can be obtained from the Intercomparison of Mid-Latitude Storm Diagnostics (IMILAST) project at https://proclim.scnat.ch/en/activities/project_imilast/data_download. Meanwhile, the composite tracks of Mediterranean cyclones from Flaounas et al. (2023) is available at https://doi.org/10.5281/zenodo.7378600.

Funding

This work is supported by the SETESTRELO project under grant no. PID2021-122314OB-I00, funded by the Ministerio de Ciencia,

Innovación y Universidades, Spain MCIN/10.13039/501100011033). Partial support was also obtained from the Xunta de Galicia under the Project ED431C 2021/44 (Programa de Consolidación e Estructuración de Unidades de Investigación Competitivas (Grupos de Referencia Competitiva) and Consellería de Cultura, Educación e Universidade).

CRediT authorship contribution statement

Albenis Pérez-Alarcón: Writing – review & editing, Writing – original draft, Visualization, Validation, Software, Methodology, Investigation, Formal analysis, Data curation, Conceptualization. **Patricia Coll-Hidalgo:** Writing – review & editing, Methodology, Conceptualization. **Ricardo M. Trigo:** Writing – review & editing, Validation, Supervision, Investigation. **Raquel Nieto:** Writing – review & editing, Supervision, Resources, Project administration, Funding acquisition. **Luis Gimeno:** Writing – review & editing, Supervision, Project administration, Funding acquisition.

Declaration of competing interest

The authors declare that they have no known competing financial interests or personal relationships that could have appeared to influence the work reported in this paper.

Data availability

We have shared the link to the code in the Software and data availability section

Acknowledgements

A.P-A. thanks the support from the Xunta de Galicia (Consellería de Cultura, Educación e Universidade) under the Postdoctoral grant No. ED481B-2023/016. P.C.-H. acknowledges the support from the Xunta de Galicia (Consellería de Cultura, Educación e Universidade) under PhD grant No. ED481A-2022/128. R.M.T was supported by the Portuguese Science Foundation (FCT) through the project AMOTHEC (DRI/India/0098/2020" title = "https://doi.org/10.54499/DRI/India/0098/2020">https://doi.org/10.54499/DRI/India/0098/2020). EPhysLab members are supported by the SETESTRELO project (grant no. PID2021-122314OB-I00) funded by the Ministerio de Ciencia, Innovación y Universidades, Spain (MCIN/10.13039/501100011033), Xunta de Galicia under the Project ED431C2021/44 (Programa de Consolidación e Estructuración de Unidades de Investigación Competitivas (Grupos de Referencia Competitiva) and Consellería de Cultura, Educación e Universidade), and 'ERDF A way of making Europe'. This work has also been possible thanks to the computing resources and technical support provided by CESGA (Centro de Supercomputación de Galicia) and RES (Red Española de Supercomputación). We also acknowledge the funding for open access from the Universidade de Vigo/Consorcio Interuniversitario do Sistema Universitario de Galicia.

Appendix A. Supplementary data

Supplementary data to this article can be found online at https://doi.org/10.1016/j.envsoft.2024.106027.

References

Accarino, G., Donno, D., Immorlano, F., Elia, D., Aloisio, G., 2023. An ensemble machine learning approach for tropical cyclone localization and tracking from ERA5 reanalysis data. Earth Space Sci. 10 (11), e2023EA003106 https://doi.org/10.1029/2023EA003106.

Akperov, M.G., Bardin, M.Y., Volodin, E.M., Golitsyn, G.S., Mokhov, I.I., 2007. Probability distributions for cyclones and anticyclones from the NCEP/NCAR reanalysis data and the INM RAS climate model. Izvestiya Atmos. Ocean. Phys. 43, 705–712. https://doi.org/10.1134/S0001433807060047.

Albert, J., Gulakaram, V.S., Vissa, N.K., Bhaskaran, P.K., Dash, M.K., 2023. Recent warming trends in the Arabian sea: causative factors and physical mechanisms. Climate 11 (2), 35. https://doi.org/10.3390/cli11020035.

Aragão, L., Porcù, F., 2022. Cyclonic activity in the Mediterranean region from a high-resolution perspective using ECMWF ERA5 dataset. Clim. Dynam. 58, 1293–1310. https://doi.org/10.1007/s00382-021-05963-x.

Baker, A.J., Schiemann, R., Hodges, K.I., Demory, M.E., Mizielinski, M.S., Roberts, M.J., et al., 2019. Enhanced climate change response of wintertime North Atlantic circulation, cyclonic activity, and precipitation in a 25-km-resolution global atmospheric model. J. Clim. 32 (22), 7763–7781. https://doi.org/10.1175/JCLI-D-19-0054.1.

Bardin, M.Y., Polonsky, A.B., 2005. North Atlantic oscillation and synoptic variability in the European-Atlantic region in winter. Izvestiya Atmos. Ocean. Phys. 41 (2), 127–136.

Benestad, R., Chen, D., 2006. The use of a calculus-based cyclone identification method for generating storm statistics. Tellus 58, 473–486. https://doi.org/10.1111/j.1600-0870.2006.00191.x.

Bell, S.S., Chand, S.S., Tory, K.J., Turville, C., 2018. Statistical assessment of the OWZ tropical cyclone tracking scheme in ERA-interim. J. Clim. 31, 2217–2232. https://doi.org/10.1175/JCLI-D-17-0548.1.

Bevacqua, E., Zappa, G., Shepherd, T.G., 2020. Shorter cyclone clusters modulate changes in European wintertime precipitation extremes. Environ. Res. Lett. 15 (12), 124005 https://doi.org/10.1088/1748-9326/abbde7.

Bié, A.J., de Camargo, R., 2023. Tropical cyclones position and intensity in the Southwest Indian Ocean as represented by CFS and ERA5 atmospheric reanalysis datasets. Int. J. Climatol. 43 (10), 4532–4551. https://doi.org/10.1002/joc.8101.

Blender, R., Fraedrich, K., Lunkeit, F., 1997. Identification of cyclone-track regimes in the North Atlantic. Q. J. R. Meteorol. Soc. 123 (539), 727–741. https://doi.org/10.1002/qj.49712353910.

Bourdin, S., Fromang, S., Dulac, W., Cattiaux, J., Chauvin, F., 2022. Intercomparison of four algorithms for detecting tropical cyclones using ERA5. Geosci. Model Dev. (GMD) 15, 6759–6786. https://doi.org/10.5194/gmd-15-6759-2022.

Campins, J., Jansà, A., Genovés, A., 2006. Three-dimensional structure of western Mediterranean cyclones. Int. J. Climatol. 26, 323–343. https://doi.org/10.1002/joc.1275.

Campins, J., Genovés, A., Picornell, M.A., Jansà, A., 2011. Climatology of Mediterranean cyclones using the ERA-40 dataset. Int. J. Climatol. 31, 1596–1614. https://doi.org/10.1002/joc.2183.

Cardoso, A.A., da Rocha, R.P., Crespo, N.M., 2022. Synoptic climatology of subtropical cyclone impacts on near-surface winds over the South Atlantic basin. Earth Space Sci. 9, e2022EA002482 https://doi.org/10.1029/2022EA002482.

Cattiaux, J., Chauvin, F., Bousquet, O., Malardel, S., Tsai, C.L., 2020. Projected changes in the Southern Indian Ocean cyclone activity assessed from high-resolution experiments and CMIP5 models. J. Clim. 33 (12), 4975–4991. https://doi.org/10.1175/JCLI-D-19-0591.1.

Cavicchia, L., von Storch, H., Gualdi, S., 2014. A long-term climatology of medicanes. Clim. Dynam. 43, 1183–1195. https://doi.org/10.1007/s00382-013-1893-7.

Chauvin, F., Royer, J.F., Déqué, M., 2006. Response of hurricane-type vortices to global warming as simulated by ARPEGE-Climat at high resolution. Clim. Dynam. 27 (4), 377–399. https://doi.org/10.1007/s00382-006-0135-7.

Chavas, D.R., Emanuel, K.A., 2010. A QuikSCAT climatology of tropical cyclone size. Geophys. Res. Lett. 37 (18) https://doi.org/10.1029/2010GL044558.

Chavas, D.R., Lin, N., Emanuel, K., 2015. A model for the complete radial structure of the tropical cyclone wind field. Part I: comparison with observed structure. J. Atmos. Sci. 72 (9), 3647–3662. https://doi.org/10.1175/JAS-D-15-0014.1.

Coll-Hidalgo, P., Pérez-Alarcón, A., Nieto, R., 2022a. Moisture sources for the precipitation of tropical-like cyclones in the Mediterranean Sea: a case of study. Atmosphere 13 (8), 1327. https://doi.org/10.3390/atmos13081327.

Coll-Hidalgo, P., Pérez-Alarcón, A., Gimeno, L., 2022b. Origin of moisture for the precipitation produced by the exceptional winter storm formed over the Gulf of Mexico in March 1993. Atmosphere 13, 1154. https://doi.org/10.3390/atmos13071154.

Crawford, A.D., Serreze, M.C., 2016. Does the summer Arctic frontal zone influence Arctic Ocean cyclone activity? J. Clim. 29 (13), 4977–4993. https://doi.org/10.1175/JCLI-D-15-0755.1.

Crawford, A.D., Schreiber, E.A., Sommer, N., Serreze, M.C., Stroeve, J.C., Barber, D.G., 2021. Sensitivity of Northern Hemisphere cyclone detection and tracking results to fine spatial and temporal resolution using ERA5. Mon. Weather Rev. 149 (8), 2581–2598. https://doi.org/10.1175/MWR-D-20-0417.1.

da Rocha, R.P., Reboita, M.S., Gozzo, L.F., Dutra, L.M.M., de Jesus, E.M., 2019. Subtropical cyclones over the oceanic basins: a review. Ann. NY Acad. Sci. 1436 (1), 138–156. https://doi.org/10.1111/nyas.13927.

de Jesus, E.M., da Rocha, R.P., Crespo, N.M., et al., 2022. Future climate trends of subtropical cyclones in the South Atlantic basin in an ensemble of global and regional projections. Clim. Dynam. 58, 1221–1236. https://doi.org/10.1007/s00382-021-05958-8.

Dean, J., Ghemawat, S., 2008. MapReduce: simplified data processing on large clusters. Commun. ACM 51 (1), 107–113. https://doi.org/10.1145/1327452.1327492.

de la Vara, A., Gutiérrez-Fernández, J., González-Alemán, J.J., Gaertner, M.A., 2021. Characterization of medicanes with a minimal number of geopotential levels. Int. J. Climatol. 41 (5), 3300–3316. https://doi.org/10.1002/joc.7020.

Dee, D.P., Uppala, S.M., Simmons, A.J., Berrisford, P., Poli, P., Kobayashi,, S., et al., 2011. The ERA-Interim reanalysis: Configuration and performance of the data assimilation system. Q.J.R. Meteorol. Soc. 137 (656), 553–597. https://doi.org/10.1002/qj.828.

Di Luca, A., Evans, J.P., Pepler, A., Alexander, L., Argüeso, D., 2014. Resolution sensitivity of cyclone climatology over eastern Australia using six reanalysis products. J. Clim. 28 (24), 9530–9549. https://doi.org/10.1175/JCLI-D-14-00645.1.

Dulac, W., Cattiaux, J., Chauvin, F., Bourdin, S., Fromang, S., 2024. Assessing the representation of tropical cyclones in ERA5 with the CNRM tracker. Clim. Dynam. 62, 223–238. https://doi.org/10.1007/s00382-023-06902-8.

Flaounas, E., Aragão, L., Bernini, L., Dafis, S., Doiteau, B., Flocas, H., et al., 2023. A composite approach to produce reference datasets for extratropical cyclone tracks: application to Mediterranean cyclones. Weather Clim. Dynam. 4, 639–661. https://doi.org/10.5194/wcd-4-639-2023.

Flaounas, E., Davolio, S., Raveh-Rubin, S., Pantillon, F., Miglietta, M.M., Gaertner, M.A., et al., 2022. Mediterranean cyclones: current knowledge and open questions on dynamics, prediction, climatology and impacts. Weather Clim. Dyn. 3 (1), 173–208. https://doi.org/10.5194/wcd-3-173-2022.

Flaounas, E., Kotroni, V., Lagouvardos, K., Flaounas, I., 2014. CycloTRACK (v1. 0)–tracking winter extratropical cyclones based on relative vorticity: sensitivity to data filtering and other relevant parameters. Geosci. Model Dev. (GMD) 7 (4), 1841–1853. https://doi.org/10.5194/gmd-7-1841-2014.

Flaounas, E., Raveh-Rubin, S., Wernli, H., Drobinski, P., Bastin, S., 2015. The dynamical structure of intense Mediterranean cyclones. Clim. Dynam. 44, 2411–2427. https://doi.org/10.1007/s00382-014-2330-2.

Flaounas, E., Kelemen, F.D., Wernli, H., Gaertner, M.A., Reale, M., Sanchez-Gomez, E., Lionello, P., Calmanti, S., Podrascanin, Z., Somot, S., Akhtar, N., Romera, R., Conte, D., 2018. Assessment of an ensemble of ocean–atmosphere coupled and uncoupled regional climate models to reproduce the climatology of Mediterranean cyclones. Clim. Dynam. 51, 1023–1040. https://doi.org/10.1007/s00382-016-3398-7.

Gaertner, M.Á., González-Alemán, J.J., Romera, R., Domínguez, M., Gil, V., Sánchez, E., et al., 2018. Simulation of medicanes over the Mediterranean Sea in a regional climate model ensemble: impact of ocean–atmosphere coupling and increased resolution. Clim. Dynam. 51, 1041–1057. https://doi.org/10.1007/s00382-016-3456-1.

Giffard-Roisin, S., Yang, M., Charpiat, G., Kumler-Bonfanti, C., Kégl, B., Monteleoni, C., 2020. Tropical cyclone track forecasting using fused deep learning from aligned reanalysis data. Front. Big Data 3, 1. https://doi.org/10.3389/fdata.2020.00001.

Gozzo, L.F., da Rocha, R.P., Reboita, M.S., Sugahara, S., 2014. Subtropical cyclones over the southwestern South Atlantic: climatological aspects and case study. J. Clim. 27, 8543–8562. https://doi.org/10.1175/JCLI-D-14-00149.1.

Gozzo, L.F., da Rocha, R.P., Gimeno, L., Drumond, A., 2017. Climatology and numerical case study of moisture sources associated with subtropical cyclogenesis over the southwestern Atlantic Ocean. J. Geophys. Res. Atmos. 122, 5636–5653. https://doi.org/10.1002/2016JD025764.

Gramcianinov, C.B., Campos, R.M., De Camargo, R., Hodges, K.I., Soares, C.G., da Silva Dias, P.L., 2020. Analysis of Atlantic extratropical storm tracks characteristics in 41 years of ERA5 and CFSR/CFSv2 databases. Ocean Eng. 216, 108111 https://doi.org/10.1016/j.oceaneng.2020.108111.

Grieger, J., Leckebusch, G.C., Raible, C.C., Rudeva, I., Simmonds, I., 2018. Subantarctic cyclones identified by 14 tracking methods, and their role for moisture transports into the continent. Tellus Dyn. Meteorol. Oceanogr. 70 (1), 1–18. https://doi.org/10.1080/16000870.2018.1454808.

Hart, R.E., 2003. A cyclone phase space derived from thermal wind and thermal asymmetry. Mon. Weather Rev. 131, 585–616. https://doi.org/10.1175/1520-0493(2003)131<0585:ACPSDF>2.0.CO;2.

Hawcroft, M.K., Shaffrey, L.C., Hodges, K.I., Dacre, H.F., 2012. How much Northern Hemisphere precipitation is associated with extratropical cyclones? Geophys. Res. Lett. 39 (24) https://doi.org/10.1029/2012GL053866.

Hersbach, H., Bell, B., Berrisford, P., Hirahara, S., Horányi, A., et al., 2020. The ERA5 global reanalysis. Q. J. R. Meteorol. Soc. 146, 1999–2049. https://doi.org/10.1002/qj.3803.

Hodges, K., Cobb, A., Vidale, P.L., 2017. How well are tropical cyclones represented in reanalysis datasets? J. Clim. 30, 5243–5264. https://doi.org/10.1175/JCLI-D-16-0557.1.

Hodges, K.I., 1994. A general method for tracking analysis and its application to meteorological data. Mon. Weather Rev. 122, 2573–2586. https://doi.org/10.1175/15200493(1994)122<2573:AGMFTA>2.0.CO;2.

Hodges, K.I., 1995. Feature tracking on the unit sphere. Mon. Weather Rev. 123, 3458–3465. https://doi.org/10.1175/15200493(1995)123<3458:FTOTUS>2.0.CO;2.

Hodges, K.I., 1999. Adaptive constraints for feature tracking. Mon.Wea. Rev. 127, 1362–1373. https://doi.org/10.1175/15200493(1999)127<1362:ACFFT>2.0.CO;2.

Hodges, K.I., Hoskins, B.J., Boyle, J., Thorncroft, C., 2003. A comparison of recent reanalysis datasets using objective feature tracking: storm tracks and tropical easterly waves. Mon. Weather Rev. 131 (9), 2012–2037. https://doi.org/10.1175/1520-0493(2003)131<2012:ACORRD>2.0.CO;2.

Hofsteenge, M.G., Graversen, R.G., Rydsaa, J.H., et al., 2022. The impact of atmospheric Rossby waves and cyclones on the Arctic sea ice variability. Clim. Dynam. 59, 579–594. https://doi.org/10.1007/s00382-022-06145-z.

Horn, M., et al., 2014. Tracking scheme dependence of simulated tropical cyclone response to idealized climate simulations. J. Clim. 27, 9197–9213. https://doi.org/10.1175/JCLI-D-14-00200.1.

Hoskins, B.J., Hodges, K.I., 2002. New perspectives on the Northern Hemisphere winter storm tracks. J. Atmos. Sci. 59 (6), 1041–1061. https://doi.org/10.1175/1520-0469(2002)059<1041:NPOTNH>2.0.CO;2.

Inatsu, M., 2009. The neighbor enclosed area tracking algorithm for extratropical wintertime cyclones. Atmos. Sci. Lett. 10 (4), 267–272. https://doi.org/10.1002/asl.238.

Klotzbach, P.J., Bell, M.M., Bowen, S.G., Gibney, E.J., Knapp, K.R., Schreck, C.J., 2020. Surface pressure a more skillful predictor of normalized hurricane damage than maximum sustained wind. Bull. Am. Meteorol. Soc. 101, E830–E846. https://doi.org/10.1175/BAMS-D-19-0062.1.

Knapp, K.R., Kruk, M.C., Levinson, D.H., Diamond, H.J., Neumann, C.J., 2010. The international best track archive for climate stewardship (IBTrACS): unifying tropical cyclone data. Bull. Am. Meteorol. Soc. 91, 363–376. https://doi.org/10.1175/2009BAMS2755.1.

Knaff, J.A., Longmore, S.P., Molenar, D.A., 2014. An objective satellite-based tropical cyclone size climatology. J. Clim. 27 (1), 455–476. https://doi.org/10.1175/JCLI-D-13-00096.1.

Kotsias, G., Lolis, C.J., Hatzianastassiou, N., Bakas, N., Lionello, P., Bartzokas, A., 2023. Objective climatology and classification of the Mediterranean cyclones based on the ERA5 data set and the use of the results for the definition of seasons. Theor. Appl. Climatol. 152 (1–2), 581–597. https://doi.org/10.1007/s00704-023-04374-8.

Kumler-Bonfanti, C., Stewart, J., Hall, D., Govett, M., 2020. Tropical and extratropical cyclone detection using deep learning. J. Appl. Meteorol. Climatol. 59 (12), 1971–1985. https://doi.org/10.1175/JAMC-D-20-0117.1.

Lai, Y., Li, J., Gu, X., Liu, C., Chen, Y.D., 2021. Global compound floods from precipitation and storm surge: hazards and the roles of cyclones. J. Clim. 34, 8319–8339. https://doi.org/10.1175/JCLI-D-21-0050.1.

Landsea, C.W., Franklin, J.L., 2013. Atlantic hurricane database uncertainty and presentation of a new database format. Mon. Weather Rev. 141, 3576–3592. https://doi.org/10.1175/MWR-D-12-00254.1.

Lionello, P., Dalan, F., Elvini, E., 2002. Cyclones in the Mediterranean region: the present and the doubled CO2 climate scenarios. Clim. Res. 22, 147–159. https://doi.org/10.3354/cr022147.

Lionello, P., Trigo, I.F., Gil, V., Liberato, M.L., Nissen, K.M., Pinto, J.G., et al., 2016. Objective climatology of cyclones in the Mediterranean region: a consensus view among methods with different system identification and tracking criteria. Tellus A: Dyn. Meteorol. Oceanogr. 68 (1), 29391. https://doi.org/10.3402/tellusa.v68.29391.

Lu, X., Yu, H., Ying, M., 2021. Western North pacific tropical cyclone database created by the China meteorological administration. Adv. Atmos. Sci. 38, 690–699. https://doi.org/10.1007/s00376-020-0211-7.

Malakar, P., Kesarkar, A.P., Bhate, J.N., Singh, V., Deshamukhya, A., 2020. Comparison of reanalysis data sets to comprehend the evolution of tropical cyclones over North Indian Ocean. Earth Space Sci. 7 (2), e2019EA000978 https://doi.org/10.1029/2019EA000978.

Marchok, T., 2021. Important factors in the tracking of tropical cyclones in operational models. J. Appl. Meteorol. Climatol. 60, 1265–1284. https://doi.org/10.1175/JAMC-D-20-0175.1.

Massey, N.R., 2016. Feature tracking in high-resolution regional climate data. Comput. Geosci. 93, 36–44. https://doi.org/10.1016/j.cageo.2016.04.015.

Miglietta, M.M., Rotunno, R., 2019. Development mechanisms for Mediterranean tropical-like cyclones (medicanes). Q. J. R. Meteorol. Soc. 145 (721), 1444–1460. https://doi.org/10.1002/qj.3503.

Munsi, A., Kesarkar, A., Bhate, J., et al., 2022. Simulated dynamics and thermodynamics processes leading to the rapid intensification of rare tropical cyclones over the North Indian Oceans. J. Earth Syst. Sci. 131, 211. https://doi.org/10.1007/s12040-022-01951-9.

Murata, A., Sasaki, H., Kawase, H., Nosaka, M., 2019. The development of a resolution-independent tropical cyclone detection scheme for high-resolution climate model simulations. J. Meteorol. Soc. Ser. II 97 (2), 519–531. https://doi.org/10.2151/jmsj.2019-035.

Murakami, H., 2014. Tropical cyclones in reanalysis data sets. Geophys. Res. Lett. 41, 2133–2141. https://doi.org/10.1002/2014GL059519.

Nastos, P.T., Karavana-Papadimou, K., Matsangouras, I.T., 2018. Mediterranean tropical-like cyclones: impacts and composite daily means and anomalies of synoptic patterns. Atmos. Res. 208, 156–166. https://doi.org/10.1016/j.atmosres.2017.10.023, 2018.

Neu, U., Akperov, M.G., Bellenbaum, N., et al., 2013. IMILAST: a community effort to intercompare extratropical cyclone detection and tracking algorithms. Bull. Am. Meteorol. Soc. 94, 529–547. https://doi.org/10.1175/BAMS-D-11-00154.1.

Pérez-Alarcón, A., Fernandez-Alvarez, J.C., Coll-Hidalgo, P., 2023a. Global increase of the intensity of tropical cyclones under global warming based on their maximum potential intensity and CMIP6 models. Environ. Process. 10, 36. https://doi.org/10.1007/s40710-023-00649-4.

Pérez-Alarcón, A., Coll-Hidalgo, P., Fernández-Alvarez, J.C., Trigo, R.M., Nieto, R., Gimeno, L., 2023b. The rare case of Hurricane Catarina (2004) over the South Atlantic Ocean: the origin of its precipitation through a Lagrangian approach. Q. J. R. Meteorol. Soc. 149 (752), 1038–1055. https://doi.org/10.1002/qj.4452.

Pérez-Alarcón, A., Sorí, R., Fernández-Alvarez, J.C., Nieto, R., Gimeno, L., 2021. Comparative climatology of outer tropical cyclone size using radial wind profiles. Weather Clim. Extrem. 33, 100366 https://doi.org/10.1016/j.wace.2021.100366.

Picornell, M.A., Jansà, A., Genovés, A., Campins, J., 2001. Automated database of mesocyclones from the HIRLAM(INM) 0.5 analyses in the Western Mediterranean. Int. J. Climatol. 21, 335–354. https://doi.org/10.1002/joc.621.

Pinto, J.G., Spangehl, T., Ulbrich, U., Speth, P., 2005. Sensitivities of a cyclone detection and tracking algorithm: individual tracks and climatology. Meteorol. Z. 14 (6), 823–838. https://doi.org/10.1127/0941-2948/2005/0068.

Pravia-Sarabia, E., Gómez-Navarro, J.J., Jiménez-Guerrero, P., Montávez, J.P., 2020. TITAM (v1. 0): the time-independent tracking algorithm for medicanes. Geosci.

Model Dev. (GMD) 13 (12), 6051–6075. https://doi.org/10.5194/gmd-13-6051-2020.
Priestley, M.D.K., Ackerley, D., Catto, J.L., Hodges, K.I., McDonald, R.E., Lee, R.W., 2020. An overview of the extratropical storm tracks in CMIP6 historical simulations. J. Clim. 33, 6315–6343. https://doi.org/10.1175/JCLI-D-19-0928.1.
Quinting, J.F., Catto, J.L., Reeder, M.J., 2018. Synoptic climatology of hybrid cyclones in the Australian region. Q. J. R. Meteorol. Soc. 145 (718), 288–302. https://doi.org/10.1002/qj.3431.
Raavi, P.H., Walsh, K.J.E., 2020. Sensitivity of tropical cyclone formation to resolution-dependent and independent tracking schemes in high-resolution climate model simulations. Earth Space Sci. 7 (3), e2019EA000906 https://doi.org/10.1029/2019EA000906.
Ragone, F., Mariotti, M., Parodi, A., von Hardenberg, J., Pasquero, C., 2018. A climatological study of Western Mediterranean Medicanes in numerical simulations with explicit and parameterized convection. Atmosphere 9, 397. https://doi.org/10.3390/atmos9100397.
Raible, C.C., Della-Marta, P.M., Schwierz, C., Wernli, H., Blender, R., 2008. Northern Hemisphere extratropical cyclones: a comparison of detection and tracking methods and different reanalyses. Mon. Weather Rev. 136, 880–897. https://doi.org/10.1175/2007MWR2143.1.
Reale, M., Lionello, P., 2013. Synoptic climatology of winter intense precipitation events along the Mediterranean coasts. Nat. Hazards Earth Syst. Sci. 13, 1707–1722. https://doi.org/10.5194/nhess-13-1707-2013.
Reale, M., Cabos Narvaez, W.D., Cavicchia, L., Conte, D., Coppola, E., et al., 2022. Future projections of Mediterranean cyclone characteristics using the Med-CORDEX ensemble of coupled regional climate system models. Clim. Dynam. 58, 2501–2524. https://doi.org/10.1007/s00382-021-06018-x.
Reboita, M.S., Da Rocha, R.P., Oliveira, D.M.D., 2019. Key features and adverse weather of the named subtropical cyclones over the Southwestern South Atlantic Ocean. Atmosphere 10 (1), 6. https://doi.org/10.3390/atmos10010006.
Roberts, M.J., Camp, J., Seddon, J., Vidale, P.L., Hodges, K., Vanniere, B., et al., 2020. Impact of model resolution on tropical cyclone simulation using the HighResMIP–PRIMAVERA multimodel ensemble. J. Clim. 33, 2557–2583. https://doi.org/10.1175/JCLI-D-19-0639.1.
Roberts, M.J., Vidale, P.L., Mizielinski, M.S., Demory, M.E., Schiemann, R., Strachan, J., et al., 2015. Tropical cyclones in the UPSCALE ensemble of high-resolution global climate models. J. Clim. 28 (2), 574–596. https://doi.org/10.1175/JCLI-D-14-00131.1.
Rohrer, M., Martius, O., Raible, C.C., Brönnimann, S., 2020. Sensitivity of blocks and cyclones in ERA5 to spatial resolution and definition. Geophys. Res. Lett. 47 (7) https://doi.org/10.1029/2019GL085582 e2019GL085582.
Romero, R., Emanuel, K., 2013. Medicane risk in a changing climate. J. Geophys. Res. Atmos. 118 (12), 5992–6001. https://doi.org/10.1002/jgrd.50475.
Rudeva, I., Gulev, S.K., 2007. Climatology of cyclone size characteristics and their changes during the cyclone life cycle. Mon. Weather Rev. 135, 2568–2587. https://doi.org/10.1175/MWR3420.1.
Sanchez-Gomez, E., Somot, S., 2018. Impact of the internal variability on the cyclone tracks simulated by a regional climate model over the Med-CORDEX domain. Clim. Dynam. 51, 1005–1021. https://doi.org/10.1007/s00382-016-3394-y.
Schenkel, B.A., Lin, N., Chavas, D., Oppenheimer, M., Brammer, A., 2017. Evaluating outer tropical cyclone size in reanalysis datasets using QuikSCAT data. J. Clim. 30 (21), 8745–8762. https://doi.org/10.1175/JCLI-D-17-0122.1.
Serreze, M.C., 1995. Climatological aspects of cyclone development and decay in the Arctic. Atmos.-Ocean 33 (1), 1–23. https://doi.org/10.1080/07055900.1995.9649522.
Shen, Z., Zhang, S., 2022. The generation mechanism of cold eddies and the related heat flux exchanges in the upper ocean during two sequential tropical cyclones. Front. Mar. Sci. 9, 1061159 https://doi.org/10.3389/fmars.2022.1061159.
Simmonds, I., Murray, R., 1991. A numerical scheme for tracking cyclone centres from digital data, part 1. Aust. Meteorol. Mag. 39, 155–166.
Sinclair, V.A., Dacre, H.F., 2019. Which extratropical cyclones contribute most to the transport of moisture in the Southern Hemisphere? J. Geophys. Res. Atmos. 124 (5), 2525–2545. https://doi.org/10.1029/2018JD028766.
Sprenger, M., Fragkoulidis, G., Binder, H., Croci-Maspoli, M., Graf, P., Grams, C.M., Knippertz, P., Madonna, E., Schemm, S., Škerlak, B., Wernli, H., 2017. Global climatologies of eulerian and Lagrangian flow features based on ERA-Interim. Bull. Am. Meteorol. Soc. 98, 1739–1748. https://doi.org/10.1175/BAMS-D-15-00299.1.
Tilinina, N., Gulev, S.K., Rudeva, I., Koltermann, P., 2013. Comparing cyclone life cycle characteristics and their interannual variability in different reanalyses. J. Clim. 26 (17), 6419–6438. https://doi.org/10.1175/JCLI-D-12-00777.1.
Tory, K.J., Chand, S.S., Dare, R.A., McBride, J.L., 2013a. An assessment of a model-, grid-, and basin-independent tropical cyclone detection scheme in selected CMIP3 global climate models. J. Clim. 26, 5508–5522. https://doi.org/10.1175/JCLI-D-12-00511.1.
Tory, K.J., Chand, S.S., Dare, R.A., McBride, J.L., 2013b. The development and assessment of a model-, grid-, and basin-independent tropical cyclone detection scheme. J. Clim. 26 (15), 5493–5507. https://doi.org/10.1175/JCLI-D-12-00510.1.
Tous, M., Zappa, G., Romero, R., Shaffrey, L., Vidale, P.L., 2016. Projected changes in medicanes in the HadGEM3 N512 high-resolution global climate model. Clim. Dynam. 47, 1913–1924. https://doi.org/10.1007/s00382-015-2941-2.
Trigo, I.F., 2006. Climatology and interannual variability of storm-tracks in the Euro-Atlantic sector: a comparison between ERA-40 and NCEP/NCAR reanalyses. Clim. Dynam. 26 (2–3), 127–143. https://doi.org/10.1007/s00382-005-0065-9.
Ullrich, P.A., Zarzycki, C.M., 2017. TempestExtremes: a framework for scale-insensitive pointwise feature tracking on unstructured grids. Geosci. Model Dev. (GMD) 10, 1069–1090. https://doi.org/10.5194/gmd-10-1069-2017.
Ullrich, P.A., Zarzycki, C.M., McClenny, E.E., Pinheiro, M.C., Stansfield, A.M., Reed, K.A., 2021. TempestExtremes v2.1: a community framework for feature detection, tracking, and analysis in large datasets. Geosci. Model Dev. (GMD) 14, 5023–5048. https://doi.org/10.5194/gmd-14-5023-2021.
Uotila, P., Vihma, T., Tsukernik, M., 2013. Close interactions between the Antarctic cyclone budget and large-scale atmospheric circulation. Geophys. Res. Lett. 40 (12), 3237–3241. https://doi.org/10.1002/grl.50560.
Vecchi, G.A., Delworth, T., Gudgel, R., Kapnick, S., Rosati, A., Wittenberg, A.T., et al., 2014. On the seasonal forecasting of regional tropical cyclone activity. J. Clim. Past 27 (21), 7994–8016. https://doi.org/10.1175/JCLI-D-14-00158.1.
Vitart, F., Stockdale, T.N., 2001. Seasonal forecasting of tropical storms using coupled GCM integrations. Mon. Weather Rev. 129 (10), 2521–2537. https://doi.org/10.1175/1520-0493(2001)129%3C2521:SFOTSU%3E2.0.CO;2.
Walsh, K.J.E., Fiorino, M., Landsea, C.W., McInnes, K.L., 2007. Objectively determined resolution-dependent threshold criteria for the detection of tropical cyclones in climate models and reanalyses. J. Clim. 20, 2307–2314. https://doi.org/10.1175/JCLI4074.1.
Wang, X.L., Feng, Y., Chan, R., Isaac, V., 2016. Inter-comparison of extra-tropical cyclone activity in nine reanalysis datasets. Atmos. Res. 181, 133–153. https://doi.org/10.1016/j.atmosres.2016.06.010.
Wang, X.L., Feng, Y., Compo, G.P., Swail, V.R., Zwiers, F.W., Allan, R.J., Sardeshmukh, P. D., 2013. Trends and low frequency variability of extra-tropical cyclone activity in the ensemble of twentieth century reanalysis. Clim. Dynam. 40, 2775–2800. https://doi.org/10.1007/s00382-012-1450-9.
Wang, X.L., Swail, V.R., Zwiers, F.W., 2006. Climatology and changes of extratropical cyclone activity: comparison of ERA-40 with NCEP–NCAR reanalysis for 1958–2001. J. Clim. 19 (13), 3145–3166. https://doi.org/10.1175/JCLI3781.1.
Wernli, H., Schwierz, C., 2006. Surface cyclones in the ERA-40 dataset (1958–2001). Part I: novel identification method and global climatology. J. Atmos. Sci. 63 (10), 2486–2507. https://doi.org/10.1175/JAS3766.1.
Xia, L., Zahn, M., Hodges, K., Feser, F., Storch, H., 2012. A comparison of two identification and tracking methods for polar lows. Tellus Dyn. Meteorol. Oceanogr. 64 (1), 17196 https://doi.org/10.3402/tellusa.v64i0.17196.
Yamaguchi, M., Chan, J.C., Moon, I.J., Yoshida, K., Mizuta, R., 2020. Global warming changes tropical cyclone translation speed. Nat. Commun. 11 (1), 47. https://doi.org/10.1038/s41467-019-13902-y.
Yang, J., Duan, Z., Chen, Y., Ou, J., 2023. Assessing parametric rainfall models in reproducing tropical cyclone rainfall characteristics. Atmos. Res. 288, 106726 https://doi.org/10.1016/j.atmosres.2023.106726.
Ying, M., Zhang, W., Yu, H., Lu, X.Q., Feng, J.X., Fan, Y.X., Zhu, Y.T., Chen, D.Q., 2014. An overview of the China Meteorological Administration tropical cyclone database. J. Atmos. Ocean. Technol. 31, 287–301. https://doi.org/10.1175/JTECH-D-12-00119.1.
Zarzycki, C.M., Ullrich, P.A., Reed, K.A., 2021. Metrics for evaluating tropical cyclones in climate data. J. Appl. Meteorol. Climatol. 60 (5), 643–660. https://doi.org/10.1175/JAMC-D-20-0149.1.
Zhang, W., Villarini, G., Scoccimarro, E., Napolitano, F., 2020. Examining the precipitation associated with medicanes in the high-resolution ERA-5 reanalysis data. Int. J. Climatol. 41, E126–E132. https://doi.org/10.1002/joc.6669.
Ziv, B., Harpaz, T., Saaroni, H., Blender, R., 2015. A new methodology for identifying daughter cyclogenesis: application for the Mediterranean Basin. Int. J. Climatol. 35, 3847–3861. https://doi.org/10.1002/joc.4250.